Available online at www.sciencedirect.com
ScienceDirect
Nuclear Physics B 769 (2007) 124–173
NUCLEAR PHYSICS B

Optimized negative dimensional integration method (NDIM) and multiloop Feynman diagram calculation

Iván González, Iván Schmidt *

Department of Physics and Center of Subatomic Studies, Universidad Técnica Federico Santa María, Valparaiso, Chile

Received 30 October 2006; accepted 26 January 2007

Available online 3 February 2007

Abstract

We present an improved form of the integration technique known as NDIM (negative dimensional integration method), which is a powerful tool in the analytical evaluation of Feynman diagrams. Using this technique we study a $\phi^3 \oplus \phi^4$ theory in $D = 4 - 2\epsilon$ dimensions, considering generic topologies of L loops and E independent external momenta, and where the propagator powers are arbitrary. The method transforms the Schwinger parametric integral associated to the diagram into a multiple series expansion, whose main characteristic is that the argument contains several Kronecker deltas which appear naturally in the application of the method, and which we call diagram presolution. The optimization we present here consists in a procedure that minimizes the series multiplicity, through appropriate factorizations in the multinomials that appear in the parametric integral, and which maximizes the number of Kronecker deltas that are generated in the process. The solutions are presented in terms of generalized hypergeometric functions, obtained once the Kronecker deltas have been used in the series. Although the technique is general, we apply it to cases in which there are 2 or 3 different energy scales (masses or kinematic variables associated to the external momenta), obtaining solutions in terms of a finite sum of generalized hypergeometric series 1 and 2 variables respectively, each of them expressible as ratios between the different energy scales that characterize the topology. The main result is a method capable of solving Feynman integrals, expressing the solutions as hypergeometric series of multiplicity $(n-1)$, where n is the number of energy scales present in the diagram.

PACS: 11.25.Db; 12.38.Bx

Keywords: Perturbation theory; Scalar integrals; Multiloop Feynman diagrams; Schwinger parameters; Negative dimension method

* Corresponding author.
E-mail addresses: ivan.gonzalez@usm.cl (I. González), ivan.schmidt@usm.cl (I. Schmidt).

0550-3213/$ – see front matter
doi:10.1016/j.nuclphysb.2007.01.031

1. Introduction

In quantum field theory the permanent contrast between experimental measurements and theoretical models has been possible due to the development of novel and powerful analytical and numerical techniques in perturbative calculations. The fundamental problem that arises in perturbation theory is the actual calculation of the loop integrals associated to the Feynman diagrams, whose solution is specially difficult since these integrals contain in general both ultraviolet (UV) and infrared (IR) divergences. Using the dimensional regularization scheme, which extends the dimensionality of space–time by adding a fractional piece ($D = 4 - 2\epsilon$), it is possible to know the behavior of such divergences in terms of Laurent expansions with respect to the dimensional regulator ϵ when it tends to zero. On the other hand, the structure of the integral associated to the diagram gets increasingly more complicated when the number of external lines, loops or energy scales is increased, and therefore finding an analytical solution is extremely difficult. Of the many different techniques [1] that have been developed in order to evaluate diagrams, we can mention: integration by parts (IBP), contour parametric integrations in terms of a Mellin–Barnes representation of the diagram, the differential equations method (DEM), etc.

In the context of the present article, and as comparison, particular mention has to be made to the Mellin–Barnes integral representation of the diagram, which is a very powerful technique for finding solutions in cases of arbitrary propagator powers. These powers can typically occur when tensorial structures are present, when in the reduction process generate scalar integrals with different powers of propagators, or when there are subtopologies associated to massless virtual particles contained in a propagator, which adds to the corrected propagator a fractional piece proportional to the dimensional regulator ϵ. Something similar happens when the integration by parts (IBP) technique is used. The Mellin–Barnes integral representation consists in transforming the momentum space representation of the diagram into a parameter space representation, written in terms of multiple contour integrals. As solution of these contour integrals one obtains generalized hypergeometric series, whose arguments can be "1" or ratios of the different energy scales that are present in the diagram, and which give information about the different kinematical regions, specified in a natural way by the convergence conditions of these functions. The most interesting aspect of these type of solutions is that they can be analyzed and expanded in terms of the dimensional regulator ϵ in the kinematical region of interest. For this purpose there are known techniques, algorithms and calculation packages [2–4].

The specific technique that is used here was suggested originally by Halliday and Ricotta [5], and it is known as NDIM (negative dimensional integration method) since it performs an analytical continuation in the dimension D to negative values. This can be done due to the fact that the loop integrals have the property of being analytical functions in arbitrary dimension. In actual practice this technique represents the diagram in terms of a multiple series whose argument contains a certain number of Kronecker deltas, and the solutions emerge naturally from evaluating the sums in the different forms that these Kronecker deltas allow. The final result can be always expressed in terms of generalized hypergeometric series. This method has been developed and used by several authors, among them A. Suzuki, A. Schmidt, E. Santos, C. Anastasiou, E. Glover and C. Oleari, in many applications to essentially 1-loop diagrams.

Since the results obtained in both the Mellin–Barnes representation of diagrams and in this technique are generalized hypergeometric functions, it is possible to compare them. In these series solutions the arguments are ratios of the different energy scales that appear in the diagram, and the parameters that characterize them are linear combinations of the propagator powers and the dimension D. In such applications it was shown that at one-loop level [6–10] this technique

is comparable in terms of the complexity of the solutions, with the one coming from the Mellin–Barnes representation. Nevertheless, in 2 or more loop cases [12–17], the conclusion is that the generalization of the formalism is not adequate since the solutions get to be complicated in two essential aspects. First, the number of terms or contributions of the obtained hypergeometric functions is very high, being for some 2-loop diagrams typically of the order of thousands; and second, the complexity of each of them increases, due to the fact that the multiplicity of summations of each hypergeometric series is also quite high and goes over the number needed to represent the solutions with respect to the number of kinematical variables that the diagram possesses. Both of these aspects make that any analytical study of the solutions to the L-loop case be very complex, and therefore it becomes impossible to identify each of the contributions associated to a specific kinematical region. Nevertheless, this technique has an important advantage, since it is much simpler to apply that the Mellin–Barnes representation, because it changes the process of solving multiple contour integrals into solving a linear system of equations, a fact which is very important when one is trying to find analytical solutions.

We have verified that in the form presented by the above mentioned authors, the application of this method to the general L-loop case is indeed very cumbersome. This can be observed in the L-linear and $(L+1)$-linear multinomials that are present in the Schwinger parametric integral, which contains a number of terms that increases rapidly when the number of loops or independent external momenta increases. Therefore the number of multiple expansions grows with respect to the number of constraints or Kronecker deltas which can be obtained from the mathematical structure of the diagram and which are an essential part of the method. In the present work we have deduced the method in a different way, and in the process found analytical solutions to L-loop diagrams which moreover can contain massive propagators, extending significantly in this manner the number the diagrams that can be treated with this technique. In our formalism it is not necessary to work with the momentum representation of the graph. We start with its Schwinger parametric representation, using for this purpose the mathematical structure of a generic L loops, N propagators and E independent external lines diagram, shown in Ref. [18], and which provides a quick and direct way of obtaining the parametric representation integrand without explicitly solving the momenta integrals. We concluded that this technique is quite powerful and has significant advantages in the evaluation of an infinite set of diagrams belonging to certain topological classes, which is something that will be shown in the specific examples that are going to be presented in this work.

Our emphasis in this work will be mainly in finding appropriate procedures for obtaining the general solutions associated to a diagram, instead of analyzing in more detail each one of them, although we do it in cases in which they are naturally related to the convergence relations of the hypergeometric series, which in turn define the kinematical regions where these series are valid. The presentation of this work is as follows: Section 2 contains a description of the algebraic components of NDIM that are required for Feynman diagram evaluation, with emphasis on the basic formulae of the method, which are related to delta Kronecker generation, topology related series expansions, and the reasons for naming this series multiregion expansion. We also explain here how to obtain in a simple way the explicit Schwinger parametric representation in the different energy scales of a general topology [18]. Finally we describe an algorithm that sums up the above in a systematic sequence of steps for solving Feynman's integrals and thus obtaining the multiregion expansion of the diagram, or which could be called presolution of the graph. In Section 3 we have considered three examples where the technique is applied systematically, starting from a simple known case until a complex one with until now unknown solutions. The first is the Bubble diagram ($E=1, N=2, L=1$), with equal mass (m) propagators. This is a basic exam-

ple, whose solutions are well known [19–21]. The following example corresponds to the diagram called CBox ($E = 3, N = 5, L = 2$), which although has known solutions [11], in the on-shell massless case this is the first time in which they have been obtained using this method. Increasing the complexity, we solve this diagram for the case of three massive propagators, which by itself is a new result. Finally we find the solution for a 4-loop propagator case ($E = 1, N = 8, L = 4$), where the idea is to show that this technique is very efficient and effective when one factorizes and expands systematically the multinomials of the parametric representation. Initially the massless propagator case is solved, and then with two massive propagators. The massless case is quite simple, since it is a diagram which is reducible loop by loop; but the second case is much more difficult, and the solution is in terms of hypergeometric series of the type ${}_9F_8$, in the variables $(p^2/4m^2)$ or its reciprocal $(4m^2/p^2)$, according to the kinematical region of interest. This result is relevant given the difficulty of obtaining it using any other method in the case of arbitrary propagator powers. In Section 4 we discuss some conceptual aspects of the integration method and about the complexity of the solutions when the number of loops L increases. We have added a Section 5 as an extension of Section 3, in which we present several topologies that contain 2 or 3 different energy scales, and where we only show the presolution in each case. Finally in the appendices we include a summary of definitions and properties of 1 and 2 variable hypergeometric functions, which appear frequently in the solutions of Feynman integrals; and also a more detailed description of the equations that support the integration method here presented, with some of its properties.

The most important aspect of this work is that we have been able to associate this technique with a certain family of L-loops topologies, with respect to which it is applied very easily and directly, with the possibility of solving a large number of Feynman diagrams, which can even contain massive propagators with arbitrary powers. This allows to extend considerably the known solutions of Feynman diagrams.

2. Mathematical foundations

In order to understand the method, we describe now its main components:

- Obtaining Schwinger's parametric representation.
- Foundations of the integration method NDIM.
- General algorithm.

2.1. The parametric representation

Let us consider a generic topology G that represents a Feynman diagram in a scalar theory, and suppose that this graph is composed of N propagators or internal lines, L loops (associated to independent internal momenta $\underline{q} = \{q_1, \ldots, q_L\}$, and E independent external momenta $\underline{p} = \{p_1, \ldots, p_E\}$. Each propagator or internal line is characterized by an arbitrary and in general different mass, $\underline{m} = \{m_1, \ldots, m_N\}$.

Using the prescription of dimensional regularization we can write the momentum integral expression that represents the diagram in $D = 4 - 2\epsilon$ dimensional Minkowski space as:

$$G = G(\underline{p}, \underline{m}) = \int \frac{d^D q_1}{i\pi^{\frac{D}{2}}} \cdots \frac{d^D q_L}{i\pi^{\frac{D}{2}}} \frac{1}{(B_1^2 - m_1^2 + i0)^{\nu_1}} \cdots \frac{1}{(B_N^2 - m_N^2 + i0)^{\nu_N}}. \tag{1}$$

In this expression the symbol B_j represents the momentum of the j propagator or internal line, which in general depends on a linear combination of external $\{\underline{p}\}$ and internal $\{\underline{q}\}$ momenta: $B_j = B_j(\underline{q}, \underline{p})$. We also define $\underline{\nu} = \{\nu_1, \ldots, \nu_N\}$ as the set of powers of the propagators, which in general can take arbitrary values. After introducing Schwinger's representation, it is possible to solve the momenta integrals in terms of Gaussian integrals. The result is Schwinger's parametric representation of the diagram associated to Eq. (1), which in the general case is given by the expression:

$$G = \frac{(-1)^{\frac{LD}{2}}}{\prod_{j=1}^{N} \Gamma(\nu_j)} \int_0^\infty d\vec{x} \frac{\exp(\sum_{j=1}^{N} x_j m_j^2) \exp(-\frac{F}{U})}{U^{\frac{D}{2}}}. \tag{2}$$

We have introduced for simplicity the following notation $d\vec{x} = dx_1 \cdots dx_N \prod_{j=1}^{N} x_j^{\nu_j - 1}$, where U and F are L-linear and $(L+1)$-linear multinomials respectively, defined in terms of determinants [18]:

$$\begin{aligned} U &= \Delta_{LL}^{(L)}, \\ F &= \sum_{i,j=1}^{E} \Delta_{(L+i)(L+j)}^{(L+1)} p_i \cdot p_j \\ &= \sum_{i=1}^{E} \Delta_{(L+i)(L+j)}^{(L+1)} p_i^2 + 2 \sum_{i=1}^{E-1} \sum_{j>i}^{E} \Delta_{(L+i)(L+j)}^{(L+1)} p_i \cdot p_j, \end{aligned} \tag{3}$$

where $\Delta_{ij}^{(k+1)}$ is the determinant defined by the equation:

$$\Delta_{ij}^{(k+1)} = \begin{vmatrix} M_{11} & \cdots & M_{1k} & M_{1j} \\ \vdots & & \vdots & \vdots \\ M_{k1} & \cdots & M_{kk} & M_{kj} \\ M_{i1} & \cdots & M_{ik} & M_{ij} \end{vmatrix}. \tag{4}$$

The matrix symmetric $\mathbf{M}$ has dimension $(L+E) \times (L+E)$, and is called initial parameters matrix. It is possible to easily built it when (1) is parametrized, and the internal products of loop momenta and external momenta are expanded, with coefficients which correspond to the elements of the matrix M_{ij}. For a better understanding of this process let us define the momentum:

$$Q_j = \begin{cases} q_j & \text{if } L \geqslant j \geqslant 1, \\ p_{j-L} & \text{if } (L+E) \geqslant j > L, \end{cases} \tag{5}$$

with the $(L+E)$-vector $\mathbf{Q} = [Q_1 Q_2 \cdots Q_{(L+E)}]^t$. Using this definition the following matrix structure is generated, as a previous step to the loop momenta integration:

$$\sum_{i=1}^{L+E} \sum_{j=1}^{L+E} Q_i M_{ij} Q_j = \mathbf{Q}^t \mathbf{M} \mathbf{Q}, \tag{6}$$

with which we finally identify the symmetric matrix $\mathbf{M}$. Let us develop briefly a simple example, for the massless one loop diagram shown in Fig. 1.

The corresponding 1-loop integral is given by the expression:

$$G = \int \frac{d^D q}{i\pi^{D/2}} \frac{1}{(q^2)((q+p)^2)}. \tag{7}$$

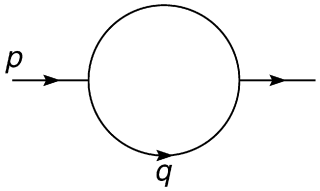

Fig. 1. Bubble diagram.

We then apply Schwinger's parametrization, and then obtain the following equation:

$$G = \int \frac{d^D q}{i\pi^{D/2}} \int_0^\infty dx_1 \exp\bigl(-x_1 q^2\bigr) \int_0^\infty dx_2 \exp\bigl(-x_2 (q+p)^2\bigr), \tag{8}$$

or equivalently, expanding the squares in the exponents and factorizing in terms of internal and external momenta, it follows that:

$$G = \int dx_1\, dx_2 \int \frac{d^D q}{i\pi^{D/2}} \exp\bigl[-\bigl[(x_1+x_2)q^2 + 2x_2 q \,.\, p + x_2 p^2\bigr]\bigr]. \tag{9}$$

Now the matrix of parameters is obtained directly from the exponent by simple observation, that is:

$$\mathbf{M} = \begin{pmatrix} x_1 + x_2 & x_2 \\ x_2 & x_2 \end{pmatrix}, \tag{10}$$

where it has been used that $Q_1 = q$ and $Q_2 = p$. Later on other examples are going to be presented. For more details see Ref. [18].

2.2. Foundations of the integration method NDIM

2.2.1. Notation and essential formulae

The exponential structure that the integral of parameters (2) presents allows that the integration method NDIM be developed and sustained by two formulae that can be deduced starting from the following integral expression:

$$\frac{1}{A^\beta} = \frac{1}{\Gamma(\beta)} \int_0^\infty dx\, x^{\beta-1} \exp(-Ax), \tag{11}$$

where the quantities A and β are in general complex. Using this equality one can justify the essential point of this method, and which is related to the equivalence (from an operational point of view) of the integration sign with a quantity which is proportional to a Kronecker delta. In order to show this we expand the integrand of Eq. (11):

$$\frac{1}{A^\beta} = \frac{1}{\Gamma(\beta)} \sum_n \frac{(-1)^n}{\Gamma(n+1)} A^n \int_0^\infty dx\, x^{\beta+n-1}. \tag{12}$$

Now the corresponding evaluation of the integral will not be done in the usual way, but we define an identity which fulfills the equality. This happens after we define the following operational

relation:

$$\int_0^\infty dx\, x^{\beta+n-1} \equiv \frac{\Gamma(\beta)\Gamma(n+1)}{(-1)^n}\delta_{\beta+n,0}. \tag{13}$$

For convenience we introduce the following notation in order to write the operational equivalent of the integral sign:

$$\int dx\, x^{\alpha+\beta-1} \equiv \langle \alpha+\beta \rangle, \tag{14}$$

where the parenthesis $\langle\cdot\rangle$ has implicit the constraint associated to the Kronecker delta and which furthermore satisfies the following property (see Appendices A–C):

$$\langle \alpha+\beta \rangle \equiv \frac{\Gamma(-\omega)\Gamma(\omega+1)}{(-1)^\omega}\delta_{\alpha+\beta,0}, \tag{15}$$

or in a simplified manner:

$$\langle \alpha+\beta \rangle = \frac{\Gamma(-\omega)}{\Phi_\omega}\delta_{\alpha+\beta,0}, \tag{16}$$

where ω is an arbitrary index or parameter and where we have also defined the factor:

$$\Phi_\omega = \frac{(-1)^\omega}{\Gamma(\omega+1)}. \tag{17}$$

On the other hand, by applying successively Eq. (11) and then Eq. (14) to an arbitrary multinomial, we can deduce the second fundamental formula on which the method is based. This expresses the fact that a multinomial of σ terms can be written as a multiregion expansion, in such a way that it simultaneously contains all limiting possible cases with respect to the relation between the different terms present in the multinomial. The series so described can be written as:

$$\begin{aligned}&(A_1+\cdots+A_\sigma)^{\pm\nu}\\ &\quad= \frac{1}{\Gamma(\mp\nu)}\sum_{n_1}\cdots\sum_{n_\sigma}\Phi_{n_1,\ldots,n_\sigma}\, A_1^{n_1}\cdots A_\sigma^{n_\sigma}\langle \mp\nu+n_1+\cdots+n_\sigma\rangle,\end{aligned} \tag{18}$$

where the terms A_i $(i=1,\ldots,\sigma)$ and the exponent ν are quantities that can take arbitrary values. The expression (18) contains the σ expansions that can be obtained and which have the general form:

$$\sim \frac{A_i^{\pm\nu}}{\Gamma(\mp\nu)}\sum_{n_j=0}^{\infty}\cdots\sum_{n_\sigma=0}^{\infty}\Phi_{n_1,\ldots,n_\sigma}\left(\frac{A_1}{A_i}\right)^{n_1}\cdots\left(\frac{A_\sigma}{A_i}\right)^{n_\sigma}\Gamma\left(\sum_{j=1}^{\sigma}n_j\mp\nu\right)\delta_{n_i,0}, \tag{19}$$

where the definition of the factor in (17) has been generalized:

$$\Phi_{n_1,\ldots,n_\sigma} = (-1)^{n_1+\cdots+n_\sigma}\frac{1}{\Gamma(n_1+1)\cdots\Gamma(n_\sigma+1)}. \tag{20}$$

In this case each of the expansions (19) that can be obtained starting from (18) correspond to multivariable generalized hypergeometric series of multiplicity $\mu=(\sigma-1)$, and each one of them contains the limiting cases or region where it is fulfilled that $(A_j/A_i<1)\ \forall j\neq i$.

2.2.2. General form of the multiregion expansion of a diagram and its solution

Once the parametric representation of a diagram (2) has been obtained, the following step is to evaluate it, and for this purpose it is necessary to make an expansion of the integrand starting from the exponential functions if they are present, and then continuing with a multiregion expansion of all the multinomials that the process generates according to formula (18). The expansion process ends when one finally obtains only one term, which is a product of all the Schwinger parameters. Now it only remains to replace all the integrals according to the formula (14) or its equivalent $\langle\cdot\rangle$. We have obtained in this manner the presolution or multiregion expansion of the Feynman integral considered in (1). In the case in which we consider a generic topology G, characterized by M different mass scales, N propagators and P Lorentz invariants associated to internal products of the external independent momenta, then the general form of the multiregion expansion is given by the following expression:

$$G = (-1)^{LD/2} \sum_{n_1,\ldots,n_\sigma} \Phi_{n_1,\ldots,n_\sigma} \prod_{j=1}^{P} \bigl(Q_j^2\bigr)^{n_j} \prod_{j=P+1}^{P+M} \bigl(-m_j^2\bigr)^{n_j} \prod_{j=1}^{N} \frac{\langle \nu_j + \alpha_j \rangle}{\Gamma(\nu_j)} \prod_{j=1}^{K} \frac{\langle \beta_j + \gamma_j \rangle}{\Gamma(\beta_j)}, \tag{21}$$

where it is possible to identify the following quantities:

$\sigma \Rightarrow$ Corresponds to the multiplicity or number of summations that conform the multiregion expansion, or in this case the presolution of the diagram G.

$Q_j^2 \Rightarrow$ Corresponds to a kinematical Lorentz invariant, which is a quadratic form of the independent external momenta.

$\alpha_j, \beta_j, \gamma_j \Rightarrow$ Correspond to linear combinations of the indexes $\{n_1, \ldots, n_\sigma\}$, with the exception of β_1, which includes a dependence on the dimension D:

$$\beta_1 = \frac{D}{2} + n_1 + \cdots + n_P. \tag{22}$$

The coefficients of the sum indexes $\{n_i\}$ in the linear combinations α_j and γ_j are $(+1)$ and in the case of β_j the indexes have coefficients (-1), except for β_1.

$N \Rightarrow$ Number of propagators or equivalently number of parametric integrations that the method transforms into N Kronecker deltas.

$K \Rightarrow$ Number related to the total number of multiregion expansions performed over the integrand of the parametric representation, which in turn generates K constraints or equivalently K Kronecker deltas.

A particular case corresponds to vacuum fluctuation diagrams, in which case the presolution (21) is written in the following form:

$$G = (-1)^{LD/2} \sum_{n_1,\ldots,n_\sigma} \Phi_{n_1,\ldots,n_\sigma} \prod_{j=1}^{M} \bigl(-m_j^2\bigr)^{n_j} \prod_{j=1}^{N} \frac{\langle \nu_j + \alpha_j \rangle}{\Gamma(\nu_j)} \prod_{j=1}^{K} \frac{\langle \beta_j + \gamma_j \rangle}{\Gamma(\beta_j)}, \tag{23}$$

where $\beta_1 = D/2$.

In order to find the solutions, it is necessary to evaluate the sums using for this purpose the existing constraints among the indexes of the sum, represented by the $\delta = (N + K)$ Kronecker deltas; but as it can be seen there are several ways to do this evaluation. In fact the number of different forms to evaluate the presolution of G using the Kronecker deltas is given by the

combinatorial formula:

$$C_{\delta}^{\sigma} = \frac{\sigma!}{\delta!(\sigma-\delta)!}. \tag{24}$$

Each one of these forms of summing using the Kronecker deltas in G, generates in turn as a result a multiple series, which corresponds to a generalized hypergeometric function, whose multiplicity is given by:

$$\mu = (\sigma - \delta). \tag{25}$$

In general it is not always possible to use the δ deltas in order to evaluate the corresponding δ sums, since this will depend on the combination of indexes with respect to which the sum should be done. If this happens, these cases are simply not considered as contributions to the solution and therefore are discarded. In those cases in which we do have a relevant expansion contribution, this corresponds to an serie representation of the set of kinematical variables that are present in the problem, in the form of ratios of the different energy scales that appear in the topology. Since the multiregion expansion (21) contains all the limits simultaneously, all the solutions that have been found are related between them by analytical continuation, which is realized implicitly by the integration method NDIM.

In practical terms the idea of the method is to generate finally an expansion that represents the diagram G, the multiregion expansion, characterized by multiplicity σ, in combination with a number δ of Kronecker deltas. Using this it is possible to find the solutions in terms of generalized hypergeometric functions of multiplicity μ. In this work we study in detail only the topologies where the μ variables of the different solutions correspond to ratios of the different $(P + M)$ energy scales present in the topology, that is when the following condition if fulfilled:

$$\mu = (P + M - 1). \tag{26}$$

2.2.3. Minimizing expansions and maximizing the number of constraints (Kronecker deltas)

This is an essential point in the improvement of the integration technique NDIM, since it explains the procedure used to find the optimal multiregion expansion of the diagram G. The idea is quite simple and it is related to the form in which the expansion of the multinomials F and U of the parametric representation (2) is done. The technique consists in the factorization of all the multinomials which are repeated 2 or more times in the integrand, without expanding them until they factorize in one term as product of the previous expansions. In the same way the process is repeated for all the submultinomials that the process generates and ends when finally one obtains one single monomial which is a product of the N Schwinger parameters. Finally applying equation (14), the integrals get associated to N Kronecker deltas.

The main result that is achieved by such a procedure is the minimization of the number of expansions, increasing the number of submultinomials that have to be expanded and since each multiregion expansion done over them generates one Kronecker delta, using formula (18) it is clear that the number of deltas is also maximized.

Let us see the following examples where it is verified that this systematic expansion indeed generates generalized hypergeometric functions of minimized multiplicity μ, and that in general less terms than in previous approaches are part of the solution of the diagram.

Example 1. Let us consider the following function:

$$g = (a_1a_2 + a_1a_3 + a_2a_4 + a_3a_4)^{\beta}, \tag{27}$$

and let us find its corresponding multiregion expansion, with and without the factorization previously indicated.

Expansion without factorization: Applying directly formula (18) to function g, one easily obtains the multiregion expansion of the function:

$$g = \sum_{n_1,\ldots,n_4} \Phi_{n_1,\ldots,n_4} a_1^{n_1+n_2} a_2^{n_1+n_3} a_3^{n_2+n_4} a_4^{n_3+n_4} \frac{\langle -\beta + n_1 + n_2 + n_3 + n_4 \rangle}{\Gamma(-\beta)}.$$

Expansion with factorization: We now reorder the function g, factorizing the multinomial in the following way:

$$g = [a_1 b + a_4 b]^{\beta}, \tag{28}$$

where $b = (a_2 + a_3)$. We have applied the previously stated idea with respect to repeated submultinomials. We now expand the binomial in (28), obtaining the following:

$$g = \sum_{n_1,n_2} \Phi_{n_1,n_2} b^{n_1+n_2} a_1^{n_1} a_4^{n_2} \frac{\langle -\beta + n_1 + n_2 \rangle}{\Gamma(-\beta)}, \tag{29}$$

in an analogous manner the binomial $b = (a_2 + a_3)$ is now expanded, which gives as result the multiregion expansion of g:

$$g = \sum_{n_1,\ldots,n_4} \Phi_{n_1,\ldots,n_4} a_1^{n_1} a_2^{n_3} a_3^{n_4} a_4^{n_2} \frac{\langle -\beta + n_1 + n_2 \rangle}{\Gamma(-\beta)} \frac{\langle -n_1 - n_2 + n_3 + n_4 \rangle}{\Gamma(-n_1 - n_2)}. \tag{30}$$

The advantage of expanding after using the factorization of repeated submultinomials can be clearly appreciated in Table 1. Notice that the multiplicity μ of the produced hypergeometric series has decreased, although the number of relevant contributions, those that correspond to a limiting case of g, has remained the same.

Example 2. Let us consider a second example, a function g which is a product of two monomials:

$$g = (a_1 + a_2)^{\alpha} (a_1 + a_2 + a_3)^{\beta}, \tag{31}$$

and find its respective multiregion expansion with and without factorization.

Expansion without factorization: We expand each multinomial separately, and then after reordering obtain the following series for g:

$$g = \sum_{n_1,\ldots,n_5} \Phi_{n_1,\ldots,n_5} a_1^{n_1+n_3} a_2^{n_2+n_4} a_3^{n_5} \frac{\langle -\alpha + n_1 + n_2 \rangle}{\Gamma(-\alpha)} \frac{\langle -\beta + n_3 + n_4 + n_5 \rangle}{\Gamma(-\beta)}. \tag{32}$$

Table 1

	Without factorization	With factorization
Multiplicity multiregion series (σ)	4	4
Kronecker deltas associated to the expansion (δ)	1	2
Multiplicity of resulting series ($\mu = \sigma - \delta$)	3	2
Possible resulting expansions (C_{δ}^{σ})	4	6
Relevant resulting expansions	4	4

Table 2

	Without factorization	With factorization
Multiplicity of multiregion series (σ)	5	4
Kronecker deltas associated to the expansion (δ)	2	2
Multiplicity of resulting series ($\mu = \sigma - \delta$)	3	2
Possible resulting expansions (C_δ^σ)	10	6
Relevant resulting expansions	6	5

Expansion with factorization: Let us now see what happens if the repeated submultinomials in (31) are factorized as follows:

$$g = b^\alpha [b + a_3]^\beta, \tag{33}$$

where $b = (a_1 + a_2)$. Then expanding the binomial, one obtains the series:

$$g = \sum_{n_1,n_2} \Phi_{n_1,n_2}\, b^{\alpha+n_1} a_3^{n_2} \frac{\langle -\beta + n_1 + n_2 \rangle}{\Gamma(-\beta)}, \tag{34}$$

and then expanding the factor $b = (a_1 + a_2)$, which finally gives us the multiregion expansion for g:

$$g = \sum_{n_1,\ldots,n_4} \Phi_{n_1,\ldots,n_4} a_1^{n_3} a_2^{n_4} a_3^{n_2} \frac{\langle -\alpha - n_1 + n_3 + n_4 \rangle}{\Gamma(-\alpha - n_1)} \frac{\langle -\beta + n_1 + n_2 \rangle}{\Gamma(-\beta)}. \tag{35}$$

The important fact is that once again the complexity of the resulting series representations gets reduced, both in the multiplicity μ and in the number of relevant contributions, as can be seen in Table 2.

Although we have presented very simple examples, they illustrate the advantages of first doing the factorization and then expanding systematically a multinomial. In these examples we verify that the multiplicity of each hypergeometric function finally obtained decreases when using the factorization procedure of repeated submultinomials, and also the number of relevant expansions obtained from the multiregion series is reduced as well.

For the particular case of Feynman integrals, the equivalent Schwinger parametric representation is composed of two multinomials, F and U, and the factorization and expansion process shown in the examples is directly applicable to them.

2.3. The algorithm

Here we present an algorithm for finding the solution of an arbitrary Feynman diagram:

1. Find Schwinger's parametric representation (2) of the Feynman diagram G, characterized by L loops, N propagators, E independent external momenta and M different masses. In general ($M \leqslant N$).
2. Minimize the number of terms of the multinomial F, reordering such that:

$$F = \sum_{i=1}^{E} \sum_{j=1}^{E} \Delta^{(L+1)}_{(L+i)(L+j)} p_i \cdot p_j = \sum_{j=1}^{P} f_j(\vec{x})\, Q_j^2, \tag{36}$$

where the factors $f_j(\vec{x})$ correspond to multinomials which depend only on Schwinger's parameters, and where Q_j^2 is a kinematical invariant which depends on the independent external

momenta. Thus the integrand of the parametric representation acquires the following structure:

$$\frac{\exp(x_1 m_1^2)\cdots\exp(x_M m_M^2)\exp(-f_1 Q_1^2/U)\cdots\exp(-f_P Q_P^2/U)}{U^{D/2}}. \tag{37}$$

In principle, assuming that all masses are different and non-vanishing, $(M+P)$ independent (between them) expansions are obtained, only associated to these exponential functions.

3. The following step is finding repeated multinomials susceptible to factorize, both in the functions $f_j(\vec{x})$ as well as in the multinomial U. For the equal masses case, before expanding the exponential which contains them, it is convenient to factorize the terms that build a multinomial already existent in the previously factorized integrand, and then one proceeds to expand such exponential.
4. Expand the multinomials until finally a single product of Schwinger's parameters is obtained. Each performed expansion will be associated to a Kronecker delta.
5. After doing all the expansions, finally it remains to replace the integral signs by its equivalent $\langle\cdot\rangle$. By doing that we add N additional Kronecker deltas. The result is the presolution of the diagram G or its equivalent multiregion expansion (21).
6. In order to find the contribution or serie representation associated to a particular combination of the μ free indexes, the most appropriate procedure is to solve the linear system corresponding to the constraints among the indexes, obtained from the Kronecker deltas, and assume that such indexes in these equations correspond to independent free variables. Thus we obtain a set of solutions for the indexes that are not free, in terms of the μ free indexes, of the parameters $\{\nu_1,\ldots,\nu_N\}$ and of the dimension D. Each of these combinations constitute a generalized hypergeometric function, whose series representation has multiplicity μ. Not all the combinations of free indexes generate a solution, in which case the associated linear system simply has no solution or equivalently the Kronecker deltas cannot eliminate the δ sums in the non-free indexes, so the quantity C_δ^σ is an upper bound with respect to the number of possible hypergeometric contributions that are present in the solution of the diagram G.
7. Repeat the previous process for the C_δ^σ forms of combining the μ indexes. Thus we obtain at most C_δ^σ hypergeometric series, which are classified according to kinematical region of interest. The solution in each kinematical region corresponds to the algebraic sum of all the contributions that have the same kinematical argument or variable. The final result is the evaluation of the diagram G in terms of all its series solutions.

3. Applications

In order to show explicitly the integration technique, let us consider three applications. The first corresponds to the evaluation of the 1-loop massive propagator. Through this simple and known problem we present the formalism and proposed notation. In the second example, the CBox diagram, it is already possible to notice the efficiency of an adequate factorization. In this case the solution is also known and has been already obtained using a different method to the one proposed here, which is useful in order to compare the simplicity of the NDIM with respect to other methods. We also generalize this problem to cases in which the solution has not been found until now. And the last example is a 4-loop diagram which has associated a very complex integral given the number of terms that are present in the polynomials F and U, and which nevertheless with an optimal factorization becomes possible to be solved, even considering one mass scale

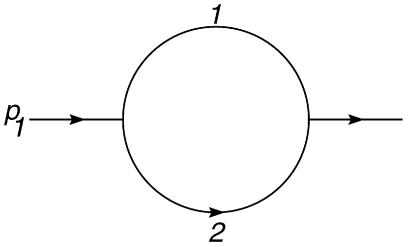

Fig. 2. Labelled bubble diagram.

in the graph. Is here where the integration technique demonstrates all its power, obtaining a completely new result and showing the simplicity of the method.

3.1. Example 1: Massive bubble diagram (Fig. 2)

This is a case in which the solutions are well known [19–21], and which we will use in order to introduce the integration method:

The integral representation of this diagram in momentum space is given by the equation:

$$G = \int \frac{d^D q_1}{i\pi^{D/2}} \frac{1}{(q_1^2 - m_1^2)^{\nu_1}((p_1 - q_1)^2 - m_2^2)^{\nu_2}}. \tag{38}$$

Let us consider the case of equal mass propagators, $m_1 = m_2 = m$, and then according to Eq. (2), the corresponding Schwinger parametric representation is given by the expression:

$$G = \frac{(-1)^{\frac{D}{2}}}{\prod_{j=1}^{2}\Gamma(\nu_j)} \int_0^\infty d\vec{x} \frac{\exp(-(x_1 + x_2)(-m^2))\exp(-\frac{x_1 x_2}{x_1 + x_2} p_1^2)}{(x_1 + x_2)^{D/2}}, \tag{39}$$

where we readily identify the multinomials of the representation, that is $U = (x_1 + x_2)$ and $F = x_1 x_2 p_1^2$. Then the only repeated multinomial coincides with U. For finding the multiregion expansion we expand first the exponentials, therefore obtaining the series:

$$G = \frac{(-1)^{\frac{D}{2}}}{\prod_{j=1}^{2}\Gamma(\nu_j)} \sum_{n_1,n_2} \Phi_{n_1,n_2} \left(p_1^2\right)^{n_1} \left(-m^2\right)^{n_2} \int d\vec{x} \frac{x_1^{n_1} x_2^{n_1}}{(x_1 + x_2)^{\frac{D}{2} + n_1 - n_2}}. \tag{40}$$

Now U is expanded:

$$\frac{1}{(x_1 + x_2)^{\frac{D}{2} + n_1 - n_2}} = \sum_{n_3,n_4} \Phi_{n_3,n_4} \frac{x_1^{n_3} x_2^{n_4}}{\Gamma(\frac{D}{2} + n_1 - n_2)} \Delta_1, \tag{41}$$

which replaced in (40) and doing a separation of integration variables gives us:

$$G = \frac{(-1)^{\frac{D}{2}}}{\prod_{j=1}^{2}\Gamma(\nu_j)} \sum_{n_1,\ldots,n_4} \Phi_{n_1,\ldots,n_4} \frac{(p_1^2)^{n_1}(-m^2)^{n_2}}{\Gamma(\frac{D}{2} + n_1 - n_2)} \Delta_1 \times \int dx_1\, x_1^{\nu_1 + n_1 + n_3 - 1} \int dx_2\, x_2^{\nu_2 + n_1 + n_4 - 1}. \tag{42}$$

Then using Eq. (14) the integrals are transformed in its equivalent $\langle\cdot\rangle$, which finally allows us to obtain the multiregion expansion of the diagram G:

$$G = \frac{(-1)^{\frac{D}{2}}}{\prod_{j=1}^{2}\Gamma(\nu_j)} \sum_{n_1,\ldots,n_4} \Phi_{n_1,\ldots,n_4} \frac{(p_1^2)^{n_1}(-m^2)^{n_2}}{\Gamma(\frac{D}{2}+n_1-n_2)} \prod_{j=1}^{3} \Delta_j, \tag{43}$$

where we have defined a notation for constraints $\{\Delta_i\}$:

$$\begin{aligned}
\Delta_1 &= \left\langle \tfrac{D}{2}+n_1-n_2+n_3+n_4 \right\rangle,\\
\Delta_2 &= \langle \nu_1+n_1+n_3\rangle,\\
\Delta_3 &= \langle \nu_2+n_1+n_4\rangle.
\end{aligned} \tag{44}$$

The number of possible representations is given by the combinatorics $C_3^4 = 4$, and the obtained hypergeometric series will have multiplicity 1. The constraints in (44) provide us with the following linear system:

$$\begin{aligned}
0 &= \tfrac{D}{2}+n_1-n_2+n_3+n_4,\\
0 &= \nu_1+n_1+n_3,\\
0 &= \nu_2+n_1+n_4.
\end{aligned} \tag{45}$$

Explicitly the combinatorics expresses that we have 3 equations and 4 variables (indexes), and therefore it is necessary to leave one free or independent index, which can be done in four different ways. Let us see this case by case:

3.1.1. Serie representation when n_1 is taken as independent index

Before doing any calculation let us define a notation for relating the index that is taken as free and the respective hypergeometric representation that it generates. For this purpose let us identify G_j as the contribution obtained once we leave index n_j free in the multiregion representation of diagram G.

Now starting form the multiregion expression (43), and using formula (16), we can replace the parenthesis $\langle\cdot\rangle$ conveniently, thus obtaining the series with index of sum n_1:

$$G_1 = \frac{(-1)^{\frac{D}{2}}}{\prod_{j=1}^{2}\Gamma(\nu_j)} \sum_{n_1} \frac{(-1)^{n_1}}{n_1!} \frac{(p_1^2)^{n_1}(-m^2)^{n_2}}{\Gamma(\frac{D}{2}+n_1-n_2)} \Gamma(-n_2)\Gamma(-n_3)\Gamma(-n_4), \tag{46}$$

where the dependent indexes (solutions of the system in (45)) take the following values:

$$\begin{aligned}
n_2 &= \tfrac{D}{2}-\nu_1-\nu_2-n_1,\\
n_3 &= -\nu_1-n_1,\\
n_4 &= -\nu_2-n_1.
\end{aligned} \tag{47}$$

Replacing now in (46), we get:

$$\begin{aligned}
G_1 = (-1)^{\frac{D}{2}} & \frac{n_1(-m^2)^{\frac{D}{2}-\nu_1+\nu_2}}{\prod_{j=1}^{2}\Gamma(\nu_j)}\\
&\times \sum_{n_1} \frac{(p_1^2/m^2)^{n_1}}{n_1!} \frac{\Gamma(\nu_1+\nu_2-\frac{D}{2}+n_1)\Gamma(\nu_1+n_1)\Gamma(\nu_2+n_1)}{\Gamma(\nu_1+\nu_2+2n_1)},
\end{aligned} \tag{48}$$

and we can then reduce the above expression in terms of a hypergeometric function:

$$G_1 = \chi_1 \big(-m^2\big)^{\frac{D}{2}-\nu_1+\nu_2}\, {}_3F_2\left(\begin{matrix} \nu_1+\nu_2-\frac{D}{2},\ \nu_1,\ \nu_2 \\ \frac{1}{2}+\frac{\nu_1+\nu_2}{2},\ \frac{\nu_1+\nu_2}{2} \end{matrix} \middle| \frac{p_1^2}{4m^2} \right), \tag{49}$$

where:

$$\chi_1 = (-1)^{D/2} \frac{\Gamma(\nu_1+\nu_2-\frac{D}{2})}{\Gamma(\nu_1+\nu_2)}. \tag{50}$$

3.1.2. Serie representation when n_2 is independent index

Analogously to the previous case, we now make the index n_2 independent, and from an adequate writing of the factors $\{\Delta_i\}$, we get the following expression associated to a free n_2:

$$G_2 = \frac{(-1)^{\frac{D}{2}}}{\prod_{j=1}^{2}\Gamma(\nu_j)} \sum_{n_2} \frac{(-1)^{n_2}}{n_2!} \frac{(p_1^2)^{n_1}(-m^2)^{n_2}}{\Gamma(\frac{D}{2}+n_1-n_2)} \Gamma(-n_1)\Gamma(-n_3)\Gamma(-n_4). \tag{51}$$

This time the solutions for the dependent indexes are given by:

$$\begin{aligned} n_1 &= \tfrac{D}{2} - \nu_1 - \nu_2 - n_2, \\ n_3 &= \nu_2 - \tfrac{D}{2} + n_2, \\ n_4 &= \nu_1 - \tfrac{D}{2} + n_2, \end{aligned} \tag{52}$$

which allows to obtain the serie representation when n_2 is free in the presolution (43):

$$G_2 = \chi_2 \big(p_1^2\big)^{\frac{D}{2}-\nu_1+\nu_2}\, {}_3F_2\left(\begin{matrix} \nu_1+\nu_2-\frac{D}{2},\ \frac{1}{2}+\frac{\nu_1+\nu_2}{2}-\frac{D}{2},\ 1+\frac{\nu_1+\nu_2}{2}-\frac{D}{2} \\ 1+\nu_1-\frac{D}{2},\ 1+\nu_2-\frac{D}{2} \end{matrix} \middle| \frac{4m^2}{p_1^2} \right), \tag{53}$$

where the prefactor χ_2 is given by the identity:

$$\chi_2 = (-1)^{\frac{D}{2}} \frac{\Gamma(\nu_1+\nu_2-\frac{D}{2})\Gamma(\frac{D}{2}-\nu_1)\Gamma(\frac{D}{2}-\nu_2)}{\Gamma(\nu_1)\Gamma(\nu_2)\Gamma(D-\nu_1-\nu_2)}.$$

3.1.3. Solution for n_3 and n_4 independent

Similar procedures to the previous ones allow us to quickly get the terms G_3 and G_4, respectively:

$$G_3 = \chi_3 \big(p_1^2\big)^{-\nu_1} \big(-m^2\big)^{\frac{D}{2}-\nu_2}\, {}_3F_2\left(\begin{matrix} \nu_1,\ \frac{1}{2}+\frac{\nu_1-\nu_2}{2},\ 1+\frac{\nu_1-\nu_2}{2} \\ 1+\nu_1-\nu_2,\ 1+\frac{D}{2}-\nu_2 \end{matrix} \middle| \frac{4m^2}{p_1^2} \right), \tag{54}$$

and

$$G_4 = \chi_4 \big(p_1^2\big)^{-\nu_2} \big(-m^2\big)^{\frac{D}{2}-\nu_1}\, {}_3F_2\left(\begin{matrix} \nu_2,\ \frac{1}{2}+\frac{\nu_2-\nu_1}{2},\ 1+\frac{\nu_2-\nu_1}{2} \\ 1+\nu_2-\nu_1,\ 1+\frac{D}{2}-\nu_1 \end{matrix} \middle| \frac{4m^2}{p_1^2} \right), \tag{55}$$

where the following factors have been defined:

$$\chi_3 = (-1)^{\frac{D}{2}} \frac{\Gamma(\nu_2-\frac{D}{2})}{\Gamma(\nu_2)}, \tag{56}$$

$$\chi_4 = (-1)^{\frac{D}{2}} \frac{\Gamma(\nu_1-\frac{D}{2})}{\Gamma(\nu_1)}. \tag{57}$$

3.1.4. Solutions in the different kinematical regions, expressed as sums of terms G_j

We can distribute the previously found solutions in the two regions where it is possible to expand the kinematical variables, the first located in $|4m^2/p_1^2| < 1$, where the solution of G is given by the expression:

$$G\left(\frac{4m^2}{p_1^2}\right) = G_2 + G_3 + G_4, \tag{58}$$

and the solution in the region where $|p_1^2/4m^2| < 1$:

$$G\left(\frac{p_1^2}{4m^2}\right) = G_1. \tag{59}$$

In this way we have evaluated G in terms of hypergeometric functions, which correspond naturally to serie representations with respect to the two energy scales present in diagram G.

3.2. Example 2: CBox diagram (on-shell case)

The next diagram of Fig. 3 has known solutions [11], found by a different method. An attempt using NDIM can be found in Ref. [22]. Nevertheless, the result presented here is an improvement in the sense that it is much simpler and easy to obtain. We do not need to use any simplification tools in order to get the final result.

For this diagram the integral representation in momentum space is given by:

$$G = \int \frac{d^D q_1}{i\pi^{\frac{D}{2}}} \frac{d^D q_2}{i\pi^{\frac{D}{2}}} \frac{1}{(B_1)^{\nu_1}} \frac{1}{(B_2)^{\nu_2}} \frac{1}{(B_3)^{\nu_3}} \frac{1}{(B_4)^{\nu_4}} \frac{1}{(B_5)^{\nu_5}}, \tag{60}$$

where the quantities B_i correspond to:

$$\begin{aligned}
B_1 &= q_1^2 - m_1^2 + i0,\\
B_2 &= (q_1 + p_1)^2 - m_2^2 + i0,\\
B_3 &= (q_1 + q_2 + p_1 + p_2)^2 - m_3^2 + i0,\\
B_4 &= (q_1 + q_2 + p_1 + p_2 + p_3)^2 - m_4^2 + i0,\\
B_5 &= q_2^2 - m_5^2 + i0.
\end{aligned} \tag{61}$$

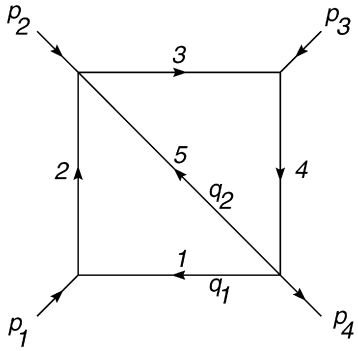

Fig. 3. Labelled CBox diagram.

According to the method developed in Ref. [18], we can find the initial parameters matrix associated to the topology, which is:

$$\mathbf{M} = \begin{pmatrix} x_1+x_2+x_3+x_4 & x_3+x_4 & x_2+x_3+x_4 & x_3+x_4 & x_4 \\ x_3+x_4 & x_3+x_4+x_5 & x_3+x_4 & x_3+x_4 & x_4 \\ x_2+x_3+x_4 & x_3+x_4 & x_2+x_3+x_4 & x_3+x_4 & x_4 \\ x_3+x_4 & x_3+x_4 & x_3+x_4 & x_3+x_4 & x_4 \\ x_4 & x_4 & x_4 & x_4 & x_4 \end{pmatrix}. \tag{62}$$

Starting from this matrix we can find the algebraic components of the parametric representation, evaluating for this purpose the polynomials U and F. The multinomial (2-lineal) U will be evaluated using the determinant:

$$\begin{aligned} U &= \begin{vmatrix} x_1+x_2+x_3+x_4 & x_3+x_4 \\ x_3+x_4 & x_3+x_4+x_5 \end{vmatrix} \\ &= x_5x_1 + x_5x_2 + x_5x_3 + x_5x_4 + x_1x_3 + x_1x_4 + x_2x_3 + x_2x_4, \end{aligned} \tag{63}$$

and the multinomial (3-lineal) F will be written as:

$$F = 2C_{1,2}p_1 \,.\, p_2 + 2C_{1,3}p_1 \,.\, p_3 + 2C_{2,3}p_2 \,.\, p_3, \tag{64}$$

where the coefficients $C_{i,j}$ are evaluated in terms of subdeterminants of the matrix of parameters, and then:

$$\begin{aligned} C_{1,2} &= \begin{vmatrix} x_1+x_2+x_3+x_4 & x_3+x_4 & x_2+x_3+x_4 \\ x_3+x_4 & x_3+x_4+x_5 & x_3+x_4 \\ x_3+x_4 & x_3+x_4 & x_3+x_4 \end{vmatrix} = x_1x_5x_3 + x_1x_5x_4, \\ C_{1,3} &= \begin{vmatrix} x_1+x_2+x_3+x_4 & x_3+x_4 & x_2+x_3+x_4 \\ x_3+x_4 & x_3+x_4+x_5 & x_3+x_4 \\ x_4 & x_4 & x_4 \end{vmatrix} = x_1x_4x_5, \\ C_{2,3} &= \begin{vmatrix} x_1+x_2+x_3+x_4 & x_3+x_4 & x_3+x_4 \\ x_3+x_4 & x_3+x_4+x_5 & x_3+x_4 \\ x_4 & x_4 & x_4 \end{vmatrix} = x_4x_5x_1 + x_4x_5x_2. \end{aligned} \tag{65}$$

We then have for F:

$$F = 2(p_1 \,.\, p_2)x_1x_3x_5 + 2(p_2 \,.\, p_3)x_2x_4x_5 + 2(p_1 \,.\, p_2 + p_1 \,.\, p_3 + p_2 \,.\, p_3)x_1x_4x_5, \tag{66}$$

but since $2(p_1 \,.\, p_2 + p_1 \,.\, p_3 + p_2 \,.\, p_3) = (p_1+p_2+p_3)^2 = p_4^2 = 0$, $2p_1 \,.\, p_2 = (p_1+p_2)^2 = s$ and $2p_2 \,.\, p_3 = (p_2+p_3)^2 = t$, we can rewrite F as:

$$F = x_1x_3x_5s + x_2x_4x_5t. \tag{67}$$

3.2.1. Massless case ($m_1 = \cdots = m_5 = 0$)

The simplest case is the one that does not consider mass scales in the diagram. In this situation the parametric representation of G has the form:

$$G = \frac{(-1)^D}{\prod_{j=1}^5 \Gamma(\nu_j)} \int_0^\infty d\vec{x} \frac{\exp(-\frac{x_1x_3x_5}{U}s)\exp(-\frac{x_2x_4x_5}{U}t)}{U^{D/2}}. \tag{68}$$

The first step is the expansion of the exponentials, after which we find:

$$G = \frac{(-1)^D}{\prod_{j=1}^5 \Gamma(\nu_j)} \sum_{n_1,n_2} \Phi_{n_1,n_2} (s)^{n_1} (t)^{n_2} \int_0^\infty d\vec{x} \frac{x_1^{n_1} x_3^{n_1} x_2^{n_2} x_4^{n_2} x_5^{n_1+n_2}}{U^{\frac{D}{2}+n_1+n_2}}. \tag{69}$$

The exponentials are not susceptible to factorization, since the exponents contain only one term. On the other hand, in order to apply the method the polynomial U is factorized in the following form:

$$U = f_1 f_2 + f_1 x_5 + f_2 x_5, \tag{70}$$

where we have defined the submultinomials:

$$f_1 = (x_1 + x_2), \qquad f_2 = (x_3 + x_4). \tag{71}$$

We now proceed to find the multiregion expansion for the factorized multinomial U, which reads:

$$\begin{aligned} \frac{1}{U^{\frac{D}{2}+n_1+n_2}} &= \frac{1}{[f_1 f_2 + f_1 x_5 + f_2 x_5]^{\frac{D}{2}+n_1+n_2}} \\ &= \sum_{n_3,\ldots,n_5} \Phi_{n_3,\ldots,n_5} \frac{(f_1)^{n_3+n_4} (f_2)^{n_3+n_5} x_5^{n_4+n_5}}{\Gamma(\frac{D}{2}+n_1+n_2)} \Delta_1, \end{aligned} \tag{72}$$

and the expansion of the submultinomials f_1 and f_2:

$$\begin{aligned} (f_1)^{n_3+n_4} &= (x_1+x_2)^{n_3+n_4} = \sum_{n_6,n_7} \Phi_{n_6,n_7} x_1^{n_6} x_2^{n_7} \frac{\Delta_2}{\Gamma(-n_3-n_4)}, \\ (f_2)^{n_3+n_5} &= (x_3+x_4)^{n_3+n_5} = \sum_{n_8,n_9} \Phi_{n_8,n_9} x_3^{n_8} x_4^{n_9} \frac{\Delta_3}{\Gamma(-n_3-n_5)}, \end{aligned} \tag{73}$$

where the constraints $\{\Delta_i\}$ are given by the following equations:

$$\begin{aligned} \Delta_1 &= \left\langle \tfrac{D}{2} + n_1 + n_2 + n_3 + n_4 + n_5 \right\rangle, \\ \Delta_2 &= \langle -n_3 - n_4 + n_6 + n_7 \rangle, \\ \Delta_3 &= \langle -n_3 - n_5 + n_8 + n_9 \rangle. \end{aligned} \tag{74}$$

Finally the multiregion expansion for U can be written as follows:

$$\frac{1}{U^{\frac{D}{2}+n_1+n_2}} = \sum_{n_3,\ldots,n_9} \Phi_{n_3,\ldots,n_9} \frac{x_1^{n_6} x_2^{n_7} x_3^{n_8} x_4^{n_9} x_5^{n_4+n_5}}{\Gamma(\frac{D}{2}+n_1+n_2)} \frac{\prod_{j=1}^3 \Delta_j}{\Gamma(-n_3-n_4)\Gamma(-n_3-n_5)}, \tag{75}$$

then replacing in (69) and separating the integration variables, we get:

$$\begin{aligned} G = \frac{(-1)^D}{\prod_{j=1}^5 \Gamma(\nu_j)} \sum_{n_1,\ldots,n_9} \Phi_{n_1,\ldots,n_9} \frac{(s)^{n_1}(t)^{n_2}}{\Gamma(\frac{D}{2}+n_1+n_2)} \frac{\prod_{j=1}^3 \Delta_j}{\Gamma(-n_3-n_4)\Gamma(-n_3-n_5)} \\ \times \int dx_1\, x_1^{n_1+n_6} \int dx_2\, x_2^{n_2+n_7} \int dx_3\, x_3^{n_1+n_8} \int dx_4\, x_4^{n_2+n_9} \int dx_5\, x_5^{n_1+n_2+n_4+n_5}, \end{aligned} \tag{76}$$

and changing the integrations by their equivalents $\langle\cdot\rangle$, we finally obtain the presolution of G:

$$G = \frac{(-1)^D}{\prod_{j=1}^5 \Gamma(\nu_j)} \sum_{n_1,\ldots,n_9} \Phi_{n_1,\ldots,n_9} \frac{(s)^{n_1}(t)^{n_2}}{\Gamma(\frac{D}{2}+n_1+n_2)} \frac{\prod_{j=1}^8 \Delta_j}{\Gamma(-n_3-n_4)\Gamma(-n_3-n_5)}, \tag{77}$$

where the constrains $\{\Delta_i\}$ associated to the integrals are:

$$\begin{aligned}
\Delta_4 &= \langle \nu_1 + n_1 + n_6 \rangle, \\
\Delta_5 &= \langle \nu_2 + n_2 + n_7 \rangle, \\
\Delta_6 &= \langle \nu_3 + n_1 + n_8 \rangle, \\
\Delta_7 &= \langle \nu_4 + n_2 + n_9 \rangle, \\
\Delta_8 &= \langle \nu_5 + n_1 + n_2 + n_4 + n_5 \rangle.
\end{aligned} \tag{78}$$

In this case we generate at most $C_8^9 = 9$ terms or contributions to the solution of G, each of which has the form ${}_l F_{(l-1)}$. Nevertheless, three of them do not contribute to the solution, and the remaining terms are distributed in two kinematical regions, which we now summarize.

Solutions in the region $|s/t| < 1$:

$$G\left(\frac{s}{t}\right) = G_1 + G_7 + G_9. \tag{79}$$

Solutions in the region $|t/s| < 1$:

$$G\left(\frac{t}{s}\right) = G_2 + G_6 + G_8. \tag{80}$$

Explicit analytical solution for the kinematical region $|s/t| < 1$. In order to compare our results with those of Ref. [11], we now present the solution which corresponds to the limit $|s/t| < 1$. The contributions that correspond to the solution of the diagram in this region are associated to the free indexes n_1, n_7 and n_9. In order to simplify the final resulting expressions we have used the following notation $\nu_{ijk\ldots} = \nu_i + \nu_j + \nu_k + \cdots$.

Explicitly the solution in this kinematical region can be written as:

$$G\left(\frac{s}{t}\right) = G_1 + G_7 + G_9, \tag{81}$$

where the contributions G_1, G_7, G_9 are given by:

$$G_1 = \chi_1 t^{D-\nu_{12345}} {}_3F_2\left(\begin{matrix} \nu_1, & \nu_3, & \nu_{12345} - D \\ 1+\nu_{1345}-D, & 1+\nu_{1235}-D \end{matrix} \middle| -\frac{s}{t} \right), \tag{82}$$

and the prefactor χ_1 corresponds to:

$$\chi_1 = (-1)^D \frac{\Gamma(\nu_{12345}-D)\Gamma(\frac{D}{2}-\nu_{12})\Gamma(\frac{D}{2}-\nu_{34})\Gamma(\frac{D}{2}-\nu_5)\Gamma(D-\nu_{1345})\Gamma(D-\nu_{1235})}{\Gamma(\nu_2)\Gamma(\nu_4)\Gamma(\nu_5)\Gamma(\frac{3D}{2}-\nu_{12345})\Gamma(D-\nu_{125})\Gamma(D-\nu_{345})}. \tag{83}$$

We also have:

$$G_7 = \chi_7 s^{D-\nu_{1345}} t^{-\nu_2} {}_3F_2\left(\begin{matrix} \nu_2, & D-\nu_{345}, & D-\nu_{145} \\ 1+D-\nu_{1345}, & 1-\nu_4+\nu_2 \end{matrix} \middle| -\frac{s}{t} \right), \tag{84}$$

where the prefactor χ_7 is:

$$\chi_7 = (-1)^D \frac{\Gamma(\frac{D}{2} - \nu_{12})\Gamma(\frac{D}{2} - \nu_{34})\Gamma(\frac{D}{2} - \nu_5)\Gamma(D - \nu_{145})\Gamma(\nu_{1345} - D)\Gamma(\nu_4 - \nu_2)}{\Gamma(\nu_1)\Gamma(\nu_3)\Gamma(\nu_4)\Gamma(\nu_5)\Gamma(\frac{3D}{2} - \nu_{12345})\Gamma(D - \nu_{125})}, \tag{85}$$

and finally:

$$G_9 = \chi_9 s^{D-\nu_{1235}} t^{-\nu_4}\, {}_3F_2\left(\begin{matrix} \nu_4, & D - \nu_{235}, & D - \nu_{125} \\ 1 + D - \nu_{1235}, & 1 - \nu_2 + \nu_4 & \end{matrix} \middle| -\frac{s}{t} \right), \tag{86}$$

with:

$$\chi_9 = (-1)^D \frac{\Gamma(\nu_{1235} - D)\Gamma(\frac{D}{2} - \nu_{12})\Gamma(\frac{D}{2} - \nu_{34})\Gamma(\frac{D}{2} - \nu_5)\Gamma(D - \nu_{235})\Gamma(\nu_2 - \nu_4)}{\Gamma(\nu_1)\Gamma(\nu_2)\Gamma(\nu_3)\Gamma(\nu_5)\Gamma(\frac{3D}{2} - \nu_{12345})\Gamma(D - \nu_{345})}. \tag{87}$$

3.2.2. Massive CBox diagram

The next level of difficulty of this problem corresponds to the addition of another energy scale in the topology. In particular let us consider associating masses of magnitude m to some of the propagators of the diagram. As a result we now obtain two-variable hypergeometric functions as solutions.

There are different alternatives for factorizing the multinomial U and extending the solution of the massless case found previously to a set of massive cases. Nevertheless, not all the possible distributions of the mass scale in the propagators generate two-variable series, and in general an arbitrary assignment of masses, even if they are equal, produces series solutions of multiplicity $\mu > 2$. The following forms of factorization of U allow us to visualize the cases in which it is possible to solve the problem in terms of two-variable series.

Factorization I.

$$U = f_1 f_2 + f_1 x_5 + f_2 x_5, \tag{88}$$

where we have defined the submultinomials:

$$f_1 = (x_1 + x_2), \qquad f_2 = (x_3 + x_4). \tag{89}$$

With this factorization it is possible to have a two-variable solution for the following massive cases:

(a)

$$m_1 = m_2 = m, \qquad m_3 = m_4 = m_5 = 0, \tag{90}$$

or

(b)

$$m_1 = m_2 = m_5 = 0, \qquad m_3 = m_4 = m. \tag{91}$$

Factorization II. Another possible factorization is given by the expression:

$$U = f_2 x_1 + f_2 x_2 + f_1 x_5, \tag{92}$$

where the submultinomials f_i are given by:

$$f_2 = (f_1 + x_5), \qquad f_1 = (x_3 + x_4), \tag{93}$$

which allows the evaluation of a more complex case, containing the following mass distribution:

$$m_1 = m_2 = 0, \qquad m_3 = m_4 = m_5 = m. \tag{94}$$

Factorization III. We can have yet another factorization of U:

$$U = f_2 x_3 + f_2 x_4 + f_1 x_5, \tag{95}$$

where we have defined:

$$f_2 = (f_1 + x_5), \qquad f_1 = (x_1 + x_2). \tag{96}$$

Such a factorization allows to consider the case when we have the following configuration:

$$m_1 = m_2 = m_5 = m, \qquad m_3 = m_4 = 0. \tag{97}$$

Obtaining the presolution in a case with massive propagators. In order to show once again the simplicity of NDIM, we will find the multiregion expansion of the diagram G associated to the following particular distribution of masses ($m_1 = m_2 = m_5 = m$) and ($m_3 = m_4 = 0$), and we will show explicitly the solution associated to a specific kinematical region. In this case the integral representation in terms of Schwinger parameters is given by:

$$G = \frac{(-1)^D}{\prod_{j=1}^5 \Gamma(\nu_j)} \int_0^\infty d\vec{x} \frac{\exp(-f_2(-m^2)) \exp(-\frac{x_1 x_3 x_5}{U} s) \exp(-\frac{x_2 x_4 x_5}{U} t)}{U^{\frac{D}{2}}}, \tag{98}$$

where the multinomial U is given by (95):

$$U = f_2 x_3 + f_2 x_4 + f_1 x_5, \tag{99}$$

with the submultinomials:

$$f_2 = (f_1 + x_5) \quad \text{and} \quad f_1 = (x_1 + x_2). \tag{100}$$

The expansion of the exponentials gives us:

$$G = \frac{(-1)^D}{\prod_{j=1}^5 \Gamma(\nu_j)} \sum_{n_1,\ldots,n_3} \Phi_{n_1,\ldots,n_3} \left(-m^2\right)^{n_1} (s)^{n_2} (t)^{n_3} \int_0^\infty d\vec{x} \, \frac{x_1^{n_2} x_2^{n_3} x_3^{n_2} x_4^{n_3} x_5^{n_2+n_3}}{U^{\frac{D}{2}+n_2+n_3}} (f_2)^{n_1}, \tag{101}$$

where the order in which the multiregion expansions to the multinomials that are present (U, f_2 and f_1) have to be made is simple, and is the following, according to the dependence level between them:

$$U(f_2, f_1) \to f_2(f_1) \to f_1.$$

A little algebra allows to finally obtain the presolution of the diagram G. Explicitly we have that:

$$G = \frac{(-1)^D}{\prod_{j=1}^5 \Gamma(\nu_j)} \sum_{n_1,\ldots,n_{10}} \Phi_{n_1,\ldots,n_{10}} \frac{(-m^2)^{n_1} (s)^{n_2} (t)^{n_3}}{\Gamma(\frac{D}{2} + n_2 + n_3)} \frac{\prod_{j=1}^8 \Delta_j}{\Gamma(-n_1 - n_4 - n_5)\Gamma(-n_6 - n_7)}, \tag{102}$$

where the following constraints have been defined:

$$\Delta_1 = \left\langle \tfrac{D}{2} + n_2 + n_3 + n_4 + n_5 + n_6 \right\rangle,$$

$$\begin{aligned}
\Delta_2 &= \langle -n_1 - n_4 - n_5 + n_7 + n_8 \rangle, \\
\Delta_3 &= \langle -n_6 - n_7 + n_9 + n_{10} \rangle, \\
\Delta_4 &= \langle \nu_1 + n_2 + n_9 \rangle, \\
\Delta_5 &= \langle \nu_2 + n_3 + n_{10} \rangle, \\
\Delta_6 &= \langle \nu_3 + n_2 + n_4 \rangle, \\
\Delta_7 &= \langle \nu_4 + n_3 + n_5 \rangle, \\
\Delta_8 &= \langle \nu_5 + n_2 + n_3 + n_6 + n_8 \rangle. \qquad (103)
\end{aligned}$$

According to this result we can say that the total number of possible contributions to the solution is $C_8^{10} = 45$, and that evidently they correspond to series of multiplicity 2. Nevertheless, 18 of these do not really contribute due to the particular nature of the linear system build from the constraints. We now show the remaining contributions, in terms of a set of components $G_{i,j}$, according to the type of two-variable hypergeometric function ($F\,{}^{p:r:u}_{q:s:v}$ or $\bar{F}\,{}^{p:r:u}_{q:s:v}$, see appendix) that is generated and also according to the arguments of this same function:

Set 1: $G_{1,5} + G_{1,10} + G_{7,10} + G_{8,10} \Rightarrow \bar{F}\left(\quad \left| \frac{4m^2}{s}, \frac{s}{t} \right. \right)$,

Set 2: $G_{5,7} + G_{5,8} \Rightarrow \bar{F}\left(\quad \left| -\frac{s}{t}, -\frac{4m^2}{s} \right. \right)$,

Set 3: $G_{1,4} + G_{1,9} + G_{7,9} + G_{8,9} \Rightarrow \bar{F}\left(\quad \left| \frac{4m^2}{t}, \frac{t}{s} \right. \right)$,

Set 4: $G_{4,7} + G_{4,8} \Rightarrow \bar{F}\left(\quad \left| -\frac{t}{s}, -\frac{4m^2}{t} \right. \right)$,

Set 5: $G_{4,5} + G_{4,10} + G_{5,9} + (G_{9,10} = 0) \Rightarrow F\left(\quad \left| \frac{4m^2}{s}, \frac{4m^2}{t} \right. \right)$,

Set 6: $G_{1,3} + G_{3,7} + G_{3,8} \Rightarrow F\left(\quad \left| \frac{4m^2}{s}, -\frac{t}{s} \right. \right)$,

Set 7: $G_{1,2} + G_{2,7} + G_{2,8} \Rightarrow F\left(\quad \left| \frac{4m^2}{t}, -\frac{s}{t} \right. \right)$,

Set 8: $G_{2,5} + G_{2,10} \Rightarrow \bar{F}\left(\quad \left| \frac{s}{4m^2}, -\frac{4m^2}{t} \right. \right)$,

Set 9: $G_{3,4} + G_{3,9} \Rightarrow \bar{F}\left(\quad \left| \frac{t}{4m^2}, -\frac{4m^2}{s} \right. \right)$,

Set 10: $G_{2,3} \Rightarrow F\left(\quad \left| \frac{s}{4m^2}, \frac{t}{4m^2} \right. \right)$.

It is important to notice that each set of contributions does not necessarily constitutes the final solution in certain kinematical region, because it is possible that for some cases the type of solutions get mixed. As an example let us consider the case where the magnitude of the variable $|t|$ is the dominant, in which case and according to the convergence conditions of each set of solutions, it will be possible to write immediately the solution in this region as the algebraic sum of the sets 1, 2, 5, 7, 8.

Now let us write explicitly one of the solutions of G. For this purpose we consider the solutions that are present in the region where $(4m^2 > |s|)$ and $(4m^2 > |t|)$, which according to the previous set is composed of only one contribution, $G_{2,3}$:

$$G\left(\frac{s}{4m^2}, \frac{t}{4m^2}\right) = G_{2,3}, \tag{104}$$

where the contribution $G_{2,3}$ refers to the series:

$$G_{2,3} = \frac{(-1)^D}{\prod_{j=1}^{5}\Gamma(\nu_j)} \sum_{n_2,n_3} \frac{(-1)^{n_2+n_3}}{n_2!n_3!} \frac{(-m^2)^{n_1}(s)^{n_2}(t)^{n_3}}{\Gamma(\frac{D}{2}+n_2+n_3)} \times \frac{\prod_{\substack{j=1\\ j\neq 2,3}}^{8} \Gamma(-n_j)}{\Gamma(-n_1-n_4-n_5)\Gamma(-n_6-n_7)}, \tag{105}$$

and where the dependent indexes take the following values:

$$\begin{aligned}
n_1 &= -\nu_{12345} + D - n_2 - n_3,\\
n_4 &= -\nu_3 - n_2,\\
n_5 &= -\nu_4 - n_3,\\
n_6 &= \nu_{34} - \tfrac{D}{2},\\
n_7 &= -\nu_{1234} + \tfrac{D}{2} - n_2 - n_3,\\
n_8 &= -\nu_{345} + \tfrac{D}{2} - n_2 - n_3,\\
n_9 &= -\nu_1 - n_2,\\
n_{10} &= \nu_2 - n_3.
\end{aligned} \tag{106}$$

Making the corresponding replacements and after a little algebra in the expression (105), we obtain the representation in terms of the Kampé de Fériet generalized hypergeometric function $\left(F\,{}^{p:r:u}_{q:s:v}\right)$:

$$G\left(\frac{s}{4m^2}, \frac{t}{4m^2}\right) = \chi\left(-m^2\right)^{D-\nu_{12345}} F\,{}^{3:2:2}_{4:0:0}\left(\begin{matrix}\{\alpha\} & \{a\} & \{c\}\\ \{\beta\} & \{-\} & \{-\}\end{matrix}\,\middle|\, \frac{s}{4m^2}, \frac{t}{4m^2}\right), \tag{107}$$

where the prefactor χ is given by:

$$\chi = (-1)^D \frac{\Gamma(\nu_{12345}-D)\Gamma(\nu_{1234}-\frac{D}{2})\Gamma(\nu_{345}-\frac{D}{2})\Gamma(\frac{D}{2}-\nu_{34})}{\Gamma(\nu_5)\Gamma(\nu_{125}+2\nu_{34}-D)\Gamma(\nu_{12})\Gamma(\frac{D}{2})}, \tag{108}$$

and where the corresponding parameters are:

$$\begin{aligned}
\alpha_1 &= \nu_{12345} - D, & \beta_4 &= \frac{1}{2} + \frac{\nu_{125}}{2} + \nu_{34} - \tfrac{D}{2},\\
\alpha_2 &= \nu_{1234} - \tfrac{D}{2}, & a_1 &= \nu_1,\\
\alpha_3 &= \nu_{345} - \tfrac{D}{2}, & a_2 &= \nu_3,\\
\beta_1 &= \nu_{12}, & c_1 &= \nu_2,\\
\beta_2 &= \tfrac{D}{2}, & c_2 &= \nu_4,
\end{aligned}$$

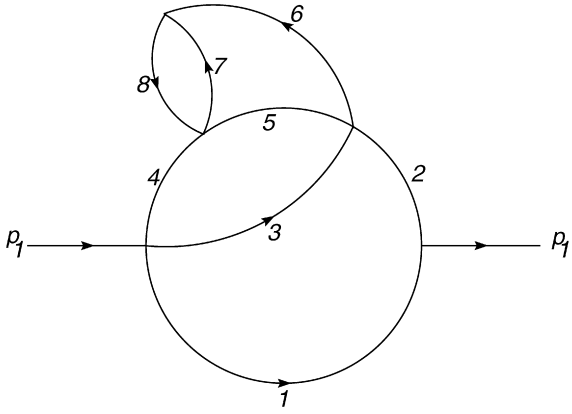

Fig. 4. Labelled four-loop propagator.

$$\beta_3 = \frac{\nu_{125}}{2} + \nu_{34} - \tfrac{D}{2}. \tag{109}$$

In this case the series converges if the following condition is satisfied:

$$\max\left\{\left|\frac{s}{4m^2}\right|, \left|\frac{t}{4m^2}\right|\right\} < 1. \tag{110}$$

3.3. Example III: Four-loop propagator

In this example the full power of the integration technique here presented is revealed, due to the fact that the parametric integral that represents the diagram of Fig. 4 is quite complex.

The integral representation in momentum space is in this case:

$$G = \int \frac{d^D q_1}{i\pi^{\frac{D}{2}}} \cdots \frac{d^D q_4}{i\pi^{\frac{D}{2}}} \prod_{j=1}^{8} \frac{1}{(k_j^2 - m_j^2 + i0)^{\nu_j}}, \tag{111}$$

where the branch momenta k_i $(i = 1, \ldots, 8)$ are respectively:

$$\begin{aligned}
k_1 &= q_1 + p_1,\\
k_2 &= q_1,\\
k_3 &= q_2 - q_1,\\
k_4 &= q_2,\\
k_5 &= q_2 - q_3,\\
k_6 &= q_3,\\
k_7 &= q_4 - q_3,\\
k_8 &= q_4.
\end{aligned} \tag{112}$$

The initial parameter matrix associated to the diagram can be easily obtained from its topology:

$$\mathbf{M} = \begin{pmatrix} x_1+x_2+x_3 & -x_3 & 0 & 0 & x_1 \\ -x_3 & x_3+x_4+x_5 & -x_5 & 0 & 0 \\ 0 & -x_5 & x_5+x_6+x_7 & -x_7 & 0 \\ 0 & 0 & -x_7 & x_7+x_8 & 0 \\ x_1 & 0 & 0 & 0 & x_1 \end{pmatrix}. \tag{113}$$

The multinomial U is obtained from the evaluation of the following determinant:

$$U = \begin{vmatrix} x_1+x_2+x_3 & -x_3 & 0 & 0 \\ -x_3 & x_3+x_4+x_5 & -x_5 & 0 \\ 0 & -x_5 & x_5+x_6+x_7 & -x_7 \\ 0 & 0 & -x_7 & x_7+x_8 \end{vmatrix},$$

$$\begin{aligned} U = {} & x_1x_3x_5x_7 + x_1x_3x_5x_8 + x_1x_3x_6x_7 + x_1x_4x_5x_7 + x_2x_3x_5x_7 \\ & + x_1x_3x_6x_8 + x_1x_4x_5x_8 + x_1x_4x_6x_7 + x_2x_3x_5x_8 + x_2x_3x_6x_7 \\ & + x_2x_4x_5x_7 + x_1x_3x_7x_8 + x_1x_4x_6x_8 + x_1x_5x_6x_7 + x_2x_3x_6x_8 \\ & + x_2x_4x_5x_8 + x_2x_4x_6x_7 + x_3x_4x_5x_7 + x_1x_4x_7x_8 + x_1x_5x_6x_8 \\ & + x_2x_3x_7x_8 + x_2x_4x_6x_8 + x_2x_5x_6x_7 + x_3x_4x_5x_8 + x_3x_4x_6x_7 \\ & + x_1x_5x_7x_8 + x_2x_4x_7x_8 + x_2x_5x_6x_8 + x_3x_4x_6x_8 + x_3x_5x_6x_7 \\ & + x_2x_5x_7x_8 + x_3x_4x_7x_8 + x_3x_5x_6x_8 + x_3x_5x_7x_8, \end{aligned} \tag{114}$$

and F is in turn obtained from the evaluation of the determinant of the expression (113):

$$\begin{aligned} F = {} & (x_1x_2x_3x_5x_7 + x_1x_2x_3x_5x_8 + x_1x_2x_3x_6x_7 + x_1x_2x_4x_5x_7 \\ & + x_1x_2x_3x_6x_8 + x_1x_2x_4x_5x_8 + x_1x_2x_4x_6x_7 + x_1x_3x_4x_5x_7 \\ & + x_1x_2x_3x_7x_8 + x_1x_2x_4x_6x_8 + x_1x_2x_5x_6x_7 + x_1x_3x_4x_5x_8 \\ & + x_1x_3x_4x_6x_7 + x_1x_2x_4x_7x_8 + x_1x_2x_5x_6x_8 + x_1x_3x_4x_6x_8 \\ & + x_1x_3x_5x_6x_7 + x_1x_2x_5x_7x_8 + x_1x_3x_4x_7x_8 + x_1x_3x_5x_6x_8 \\ & + x_1x_3x_5x_7x_8)\,p_1^2. \end{aligned} \tag{115}$$

3.3.1. Factorization of the multinomials U and F

The large number of terms that U(34) and F(21) have makes impossible to get manageable solutions if the method is applied without performing the necessary factorizations first. Nevertheless, this type of diagrams that in the massless case are solvable loop-by-loop, present a form such that they can be easily factorized in submultinomials. For this particular case the adequate multinomial factorization is:

$$F = x_1 f_7 p_1^2, \qquad U = x_1 f_6 + f_7, \tag{116}$$

where the functions f_i are given by the equations:

$$\begin{aligned} f_7 &= (x_2 f_6 + f_5), \\ f_6 &= x_3 f_4 + (x_4 f_4 + f_3), \\ f_5 &= x_3(x_4 f_4 + f_3), \\ f_4 &= x_5 f_2 + (x_6 f_2 + f_1), \end{aligned}$$

$$f_3 = x_5(x_6 f_2 + f_1),$$
$$f_2 = (x_7 + x_8),$$
$$f_1 = x_7 x_8. \tag{117}$$

3.3.2. Massless case ($m_1 = \cdots = m_8 = 0$)

This case is simple to solve loop by loop, but the advantage of the technique NDIM is that it is possible to solve the corresponding Feynman integral considering simultaneously all the loops. The parametric representation of his diagram is:

$$G = \frac{(-1)^{2D}}{\prod_{j=1}^{8}\Gamma(\nu_j)} \int_0^\infty d\vec{x} \frac{\exp(-\frac{x_1 f_7}{x_1 f_6 + f_7} p_1^2)}{(x_1 f_6 + f_7)^{D/2}}, \tag{118}$$

where as usual the exponential is expanded, and systematically we make the successive multiregion expansions associated to the multinomials f_i. The order in which these multinomials appear and get expanded is:

$$U \to f_7 \to f_6 \to f_5 \to f_4 \to f_3 \to f_2. \tag{119}$$

Once the integration process finishes, finally the presolution or multiregion expansion of the diagram G is obtained:

$$G = \frac{(-1)^{2D}}{\prod_{j=1}^{8}\Gamma(\nu_j)} \sum_{n_1,\ldots,n_{15}} \Phi_{n_1,\ldots,n_{15}} \frac{(p_1^2)^{n_1}}{\Gamma(\frac{D}{2}+n_1)} \Omega_{\{n\}} \prod_{j=1}^{15} \Delta_j, \tag{120}$$

where we have defined the factor:

$$\Omega_{\{n\}} = \big\{\Gamma(-n_1 - n_3)\Gamma(-n_2 - n_4)\Gamma(-n_5 - n_7)\Gamma(-n_6 - n_8)\Gamma(-n_9 - n_{11}) \times \Gamma(-n_{10} - n_{12})\big\}^{-1}, \tag{121}$$

and the corresponding constraints are:

$$\begin{aligned}
\Delta_1 &= \big\langle \frac{D}{2} + n_1 + n_2 + n_3 \big\rangle, & \Delta_9 &= \langle \nu_2 + n_4 \rangle,\\
\Delta_2 &= \langle -n_1 - n_3 + n_4 + n_5 \rangle, & \Delta_{10} &= \langle \nu_3 + n_5 + n_6 \rangle,\\
\Delta_3 &= \langle -n_2 - n_4 + n_6 + n_7 \rangle, & \Delta_{11} &= \langle \nu_4 + n_8 \rangle,\\
\Delta_4 &= \langle -n_5 - n_7 + n_8 + n_9 \rangle, & \Delta_{12} &= \langle \nu_5 + n_9 + n_{10} \rangle,\\
\Delta_5 &= \langle -n_6 - n_8 + n_{10} + n_{11} \rangle, & \Delta_{13} &= \langle \nu_6 + n_{12} \rangle,\\
\Delta_6 &= \langle -n_9 - n_{11} + n_{12} + n_{13} \rangle, & \Delta_{14} &= \langle \nu_7 + n_{13} + n_{14} \rangle,\\
\Delta_7 &= \langle -n_{10} - n_{12} + n_{14} + n_{15} \rangle, & \Delta_{15} &= \langle \nu_8 + n_{13} + n_{15} \rangle,\\
\Delta_8 &= \langle \nu_1 + n_1 + n_2 \rangle.
\end{aligned} \tag{122}$$

The number of possible contributions that the solution has is $C_{15}^{15} = 1$, and it does not correspond to a series but to a single term. The solution for this case is simply:

$$G = (-1)^{2D} \frac{(p_1^2)^{n_1}}{\Gamma(D/2 + n_1)} \Omega_{\{n\}} \frac{\prod_{j=1}^{15}\Gamma(-n_j)}{\prod_{j=1}^{8}\Gamma(\nu_j)}, \tag{123}$$

where the indexes n_i are to be replaced by the values:

$$
\begin{aligned}
n_1 &= 2D - \nu_1 - \nu_2 - \nu_3 - \nu_4 - \nu_5 - \nu_6 - \nu_7 - \nu_8, & n_9 &= D - \nu_5 - \nu_6 - \nu_7 - \nu_8,\\
n_2 &= \nu_2 + \nu_3 + \nu_4 + \nu_5 + \nu_6 + \nu_7 + \nu_8 - 2D, & n_{10} &= \nu_6 + \nu_7 + \nu_8 - D,\\
n_3 &= \nu_1 - \tfrac{D}{2}, & n_{11} &= \nu_5 - \tfrac{D}{2},\\
n_4 &= -\nu_2, & n_{12} &= -\nu_6,\\
n_5 &= \tfrac{3D}{2} - \nu_3 - \nu_4 - \nu_5 - \nu_6 - \nu_7 - \nu_8, & n_{13} &= \tfrac{D}{2} - \nu_7 - \nu_8,\\
n_6 &= \nu_4 + \nu_5 + \nu_6 + \nu_7 + \nu_8 - \tfrac{3D}{2}, & n_{14} &= \nu_8 - \tfrac{D}{2},\\
n_7 &= \nu_3 - \tfrac{D}{2}, & n_{15} &= \nu_7 - \tfrac{D}{2},\\
n_8 &= -\nu_4. & &
\end{aligned}
\tag{124}
$$

3.3.3. A massive case example ($m_1 = \cdots = m_6 = 0$) ($m_7 = m_8 = m$)

Let us consider a more complicated situation, which adds one energy scale m to the previous problem, as it is shown in Fig. 5. Starting from the parametric representation of the diagram:

$$
G = \frac{(-1)^{2D}}{\prod_{j=1}^{8}\Gamma(\nu_j)} \int_0^\infty d\vec{x}\, \frac{\exp(-f_2(-m^2))\exp(-\frac{x_1 f_7}{x_1 f_6 + f_7} p_1^2)}{(x_1 f_6 + f_7)^{\frac{D}{2}}},
\tag{125}
$$

and remembering that $f_2 = (x_7 + x_8)$, we proceed to make the expansions, similar to the massless case, except that this time an extra expansion appears, due to the exponential that contains the mass scale, and which gets expanded later on in the process or replacing the functions f_i. At the end of the procedure we obtain as presolution the following expression:

$$
G = \frac{(-1)^{2D}}{\prod_{j=1}^{8}\Gamma(\nu_j)} \sum_{n_1,\ldots,n_{16}} \Phi_{n_1,\ldots,n_{16}} \frac{(p_1^2)^{n_1}(-m^2)^{n_{14}}}{\Gamma(\frac{D}{2} + n_1)} \Omega_{\{n\}} \prod_{j=1}^{15} \Delta_j,
\tag{126}
$$

where $\Omega_{\{n\}}$ is the factor:

$$
\begin{aligned}
\Omega_{\{n\}} = \big\{ &\Gamma(-n_1 - n_3)\Gamma(-n_2 - n_4)\Gamma(-n_5 - n_7)\Gamma(-n_6 - n_8)\Gamma(-n_9 - n_{11})\\
&\times \Gamma(-n_{10} - n_{12} - n_{14}) \big\}^{-1}.
\end{aligned}
\tag{127}
$$

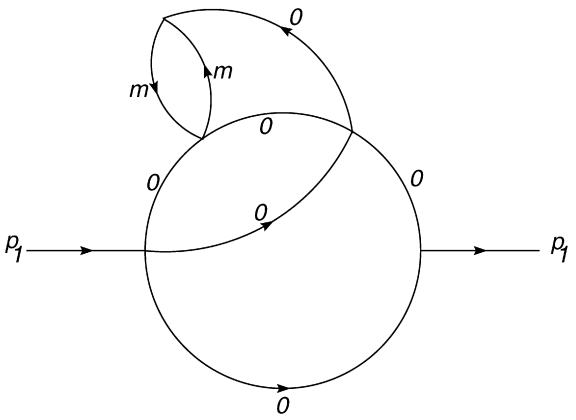

Fig. 5. Mass configuration in the four-loop propagator.

The new set of constraints $\{\Delta_j\}$, is given by the following identities:

$$\begin{aligned}
&\Delta_1 = \left\langle \tfrac{D}{2} + n_1 + n_2 + n_3 \right\rangle, && \Delta_9 = \langle \nu_2 + n_4 \rangle,\\
&\Delta_2 = \langle -n_1 - n_3 + n_4 + n_5 \rangle, && \Delta_{10} = \langle \nu_3 + n_5 + n_6 \rangle,\\
&\Delta_3 = \langle -n_2 - n_4 + n_6 + n_7 \rangle, && \Delta_{11} = \langle \nu_4 + n_8 \rangle,\\
&\Delta_4 = \langle -n_5 - n_7 + n_8 + n_9 \rangle, && \Delta_{12} = \langle \nu_5 + n_9 + n_{10} \rangle,\\
&\Delta_5 = \langle -n_6 - n_8 + n_{10} + n_{11} \rangle, && \Delta_{13} = \langle \nu_6 + n_{12} \rangle,\\
&\Delta_6 = \langle -n_9 - n_{11} + n_{12} + n_{13} \rangle, && \Delta_{14} = \langle \nu_7 + n_{13} + n_{15} \rangle,\\
&\Delta_7 = \langle -n_{10} - n_{12} - n_{14} + n_{15} + n_{16} \rangle, && \Delta_{15} = \langle \nu_8 + n_{13} + n_{16} \rangle,\\
&\Delta_8 = \langle \nu_1 + n_1 + n_2 \rangle. &&
\end{aligned} \tag{128}$$

According to the previous analysis the number of possible contributions to the solution of G is $C_{15}^{16} = 16$, of which actually only ten contribute to the final solution. These can be distributed in the following manner, taking into account the kinematical region of interest:

Solutions in the region $|p_1^2/4m^2| < 1$:

$$G\left(\frac{p_1^2}{4m^2}\right) = G_1 + G_5 + G_9 + G_{13}. \tag{129}$$

Solutions in the region $|4m^2/p_1^2| < 1$:

$$G\left(\frac{4m^2}{p_1^2}\right) = G_2 + G_6 + G_{10} + G_{14} + G_{15} + G_{16}. \tag{130}$$

4. Comments

4.1. The factorization process

From the point of view of the actual procedure the aspect that optimizes the method has to do with how the multinomials that appear in Schwinger's parametric integral are factorized. Is in this process where resides the possibility that the integration method be generalized to L loops for both massless and massive diagrams. In this respect we worked out a procedure that allows for an adequate factorization of the multinomials U and F at the moment in which they are generated, which is something very useful since without it the number of sums of these multinomials can be quite large, depending on the number of loops and external lines that the topology has.

In this work we have treated cases in which the multiplicity of the series that conform the solution fulfills the condition $\mu = (n-1)$, where n is the number of different energy scales present in the diagram. With this criterion we have classified in three families the topologies considered here, and for each case we give the recipe to factorize the multinomials U and F.

4.1.1. Diagrams reducible recursively loop by loop

The topologies that are included in this category are those that in the case in which the theory does not contain masses, they can be evaluated loop-by-loop by successive application of the formula corresponding to the 1-loop diagram:

$$G = \int \frac{d^D q_1}{i\pi^{D/2}} \frac{1}{(q_1^2)^{a_1}((q_1+p_1)^2)^{a_2}}, \tag{131}$$

whose explicit solution is:

$$G = g(a_1, a_2)\frac{1}{(p^2)^{a_1+a_2-D/2}}, \tag{132}$$

where the factor $g(a_1, a_2)$ is defined as:

$$g(a_1, a_2) = (-1)^{\frac{D}{2}}\frac{\Gamma(a_1 + a_2 - \frac{D}{2})\Gamma(\frac{D}{2} - a_1)\Gamma(\frac{D}{2} - a_2)}{\Gamma(a_1)\Gamma(a_2)\Gamma(D - a_1 - a_2)}. \tag{133}$$

The formulae (131) and (132) can be represented graphically as shown in Fig. 6.

A situation that happens quite often together with the loop by loop reduction is when there are two scalar propagators in series and associated to the same mass scale, with powers a_1 and a_2 in the propagators. In this case such powers can be summed and replaced by only one, characterized by the power $(a_1 + a_2)$. Graphically this is represented in Fig. 7.

The massless diagrams which applying formula (132) can be evaluated recursively loop by loop, are also capable of evaluation considering all loops simultaneously and even if different mass scales are added to the topology. That this can be done depends only on finding the optimal factorization of U and F. For this purpose we use the well known topological analogy between Feynman diagram and resistive electrical circuits, in the sense that in both "something" flows in their branches and "something" is conserved in their vertices. But this analogy goes further, since electrical resistors in an electrical network are equivalent to Schwinger's parameters in Feynman diagrams. The analogy is obvious if we observe Fig. 8.

In this example the following can be seen: in the Feynman diagram one finds that the ratio between the multinomials F and U is given by the expression:

$$\frac{F}{U} = \frac{x_1 x_2}{x_1 + x_2} \Rightarrow F = x_1 x_2 \wedge U = x_1 + x_2. \tag{134}$$

For simplicity we have taken $p^2 = 1$, since the results are independent of this choice. Similarly the equivalent resistance of the electrical circuit shown if the figure can be easily evaluated, giving:

$$R_{\text{eq}} = \frac{R_1 R_2}{R_1 + R_2}. \tag{135}$$

The resemblance of these mathematical structures and also considering the graphic equations shown above, allow us to explain the reason why a massless L-loop Feynman diagram can be reduced loop by loop in the same way that a resistive circuit can be reduced in terms of sums of series and parallel resistors. Both systems have the same topological characteristics. Therefore,

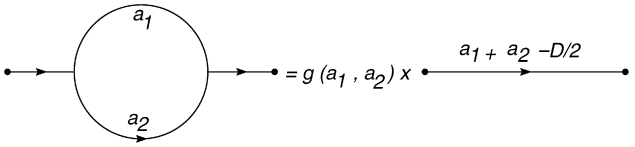

Fig. 6. Graphic formula for Bubble diagram.

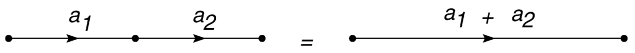

Fig. 7. Reduction of propagators in serie.

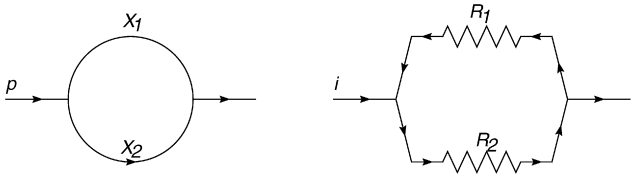

Fig. 8. Simple analogy of Feynman diagram and network of resistances.

using this similitude it is possible to think in doing "sums of parameters" depending on whether we have series or parallel propagators, and with this it is possible to find the ratio (F/U) and thus identify directly the multinomials F and U. Nevertheless, the main advantage is not really the determination of these multinomials, but the fact that in this way it is possible to find simultaneously the adequate factorization for the diagrams solvable directly and recursively loop by loop, since in the process of reducing the diagram in terms of series and parallel branches, the factorizations of the type $(x_i + x_j + \cdots + x_k)$, adequate for the application of NDIM, are generated automatically. This is the trick used in the example (III) in order to find the factorizations. A particular case are vacuum fluctuation diagrams, for which the multinomial F vanishes, and therefore for finding U it becomes necessary to assume that the diagram corresponds to a propagator, and for that purpose we adequately add two external lines, in such a way that the topology be reducible loop-by-loop. Then the same recipe as above is applied, the ratio (F/U) is determined and finally the already factorized multinomial U is found.

Notice that the factorizations of the type $(x_i + x_j + \cdots + x_k)$ contain the parameters that belong to the same loop (once the subtopologies of the loop propagators have been reduced), which seems natural since the series-parallel reduction can be done one loop at the time. It is also worth pointing out that it is possible to do this "parameters reduction" independently on whether the propagators are massless or massive, which is due to the fact that the mass scales do not appear in the multinomials U and F of the parametric integral. Moreover, it is thus clear that when adding equal mass scales, these can only be associated to the same loop, and therefore we can be sure that the series solutions increase the multiplicity in one unit, which is logical since one more mass scale has been added. As an example, if in the multinomials the factor $(x_i + x_j + \cdots + x_k)$ appears, it is possible to add to the topology equal masses in various possible situations and associate to the integral of parameters the following exponential factors:

$$\exp\bigl(x_i m^2\bigr), \quad \exp\bigl((x_i + x_j)m^2\bigr), \quad \exp\bigl((x_i + x_j + \cdots + x_k)m^2\bigr), \quad \text{etc.}$$

In the case in which equal masses are distributed in different loops, in most situations it will not be possible to factorize adequately the multinomials and the integration method will generate extra sums in the series solutions, whose arguments would be 1. The way to think about this is that when masses are put into different loops this really corresponds to different mass scales and therefore the multiplicity of the series solution will grow with the different number of mass scales in the problem.

4.1.2. Two loop topologies, with 3 or more external lines

For topologies with more than two external lines, the previous trick is not useful. Nevertheless, there is still a generic procedure that can provide an optimal factorization for the multinomial U, which in this case is the one that determines and conditions the adequate factorization that must be done in F. This procedure can be applied in general to any 2-loop diagram, although only in certain topologies optimal results are obtained, according to the criteria expressed in (26).

In actual practice the factorization of U is done directly from the matrix of parameters of the diagram, and since we are considering the two loop case, U is obtained from the determinant of the 2×2 symmetric submatrix that relates the loop momenta only. The general structure of the determinant is given by the expression:

$$U = \begin{vmatrix} X_a + X_b & \pm X_b \\ \pm X_b & X_b + X_c \end{vmatrix}, \tag{136}$$

where the terms X_a and X_c are 1-linear combinations of Schwinger parameters, such that they do not contain common parameters among them, that is $\{X_a\} \cap \{X_c\} = \varnothing$. The term X_b is a combination of the parameters that are common in the diagonal elements.

The form of U comes from the determinant of this matrix, that is:

$$U = X_a X_b + X_b X_c + X_a X_c, \tag{137}$$

where we can do the following factorizations in case they are necessary:

$$U = (X_a + X_c) X_b + X_a X_c, \tag{138}$$

$$U = X_a X_b + X_c (X_a + X_c), \tag{139}$$

$$U = X_a (X_b + X_c) + X_b X_c. \tag{140}$$

When adding one more mass scale, the appropriate factorization will depend on the form in which this scale gets distributed, and them in the integrand the following factor appears:

$$\exp\bigl(X_a m^2\bigr), \quad \exp\bigl((X_a + X_c) m^2\bigr), \quad \text{etc.}$$

This provides us with a general recipe for the case of 2-loop diagrams and more than two external points. In our work only three topologies are suitable for applying the method and producing optimal solutions, that is they fulfill the condition that the solution multiplicity is less than the number of energy scales of the diagram. These are indicated in Fig. 9.

4.1.3. The previous topologies + propagator insertions of loop by loop reducible topologies

The last case we will consider is a combination of the two-loop topologies shown in Fig. 9, with the addition of subgraphs in the loop-by-loop reducible propagators, and with the advantage that it is also possible to include masses in them. In this manner it becomes possible to extend to L-loops the two-loop topologies shown previously.

4.2. Increase in complexity of the hypergeometric series as the number of loops L grows

In this work we have applied the method to certain L-loop class of diagrams characterized for having 1, 2 or 3 different energy scales, and such that the solutions correspond only to series of 0, 1 or 2 variables respectively.

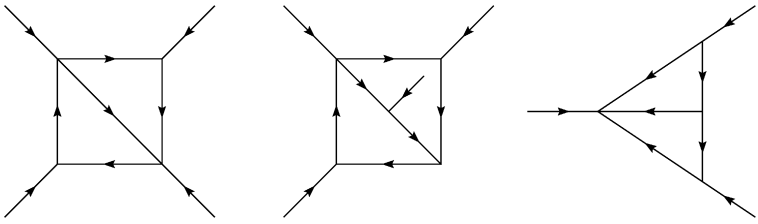

Fig. 9. Two loops diagrams compatible with NDIM.

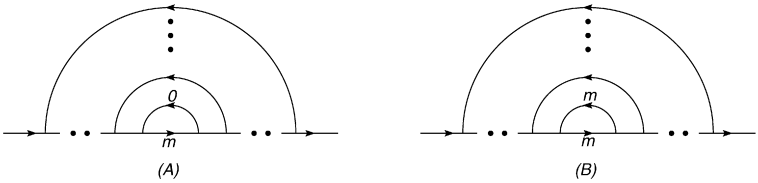

Fig. 10. Two massive family of L loops propagators.

With this restriction in the type of solution, the topologies to which is possible to apply the technique NDIM advantageously are the following:

- One loop topologies with 2, 3 and 4 external points, which have been studied in Refs. [6,10].
- All L-loop topologies of two external points which are loop by loop recursively reducible in the massless propagators case, but to which 1 or 2 mass scales are added.
- All L-loop vacuum fluctuation topologies that are reducible loop by loop, and to which up to 3 different energy scales can be added.
- Some 2-loop diagrams, shown in Fig. 9.

To all these topologies more loops can be added by including 1-loop insertions in the propagators, and since it is also possible to assign mass to these insertions, we can therefore study a great variety of graphs with this integration technique. In conclusion a large family of L-loop diagrams can be evaluated with this method.

Our results indicate that the number of parameters that characterize the generalized hypergeometric functions that are obtained as solutions to the diagrams increases linearly with the number of loops L of the graph. In the case of topologies that have two energy scales, the solutions are always expressible as generalized hypergeometric series of the type ${}_lF_{l-1}$, where l corresponds to the hypergeometric order and the quantity $(2l-1)$ is the total number of parameters that it has. Let us see how the number of loops L affects the order of the hypergeometric series in the solution. We consider the following examples which are associated to the diagram in Fig. 10, and which have 2 different energy scales $\{p^2, m^2\}$ and L loops. For this class of diagrams we show 2 topologies which have masses associated to one of the loops, with the difference that while the first (A) has one massive propagator the second (B) has both propagators massive, and the rest of the propagators are massless.

The solutions that we have found for these diagrams are given in terms of generalized hypergeometric functions ${}_lF_{l-1}$, where the graphs with the condition (A) have series solutions of the form:

$$
{}_{2L}F_{(2L-1)}\left(\cdots\left|\frac{p^2}{m^2}\right.\right),
$$

$$
{}_{2L}F_{(2L-1)}\left(\cdots\left|\frac{m^2}{p^2}\right.\right),
$$

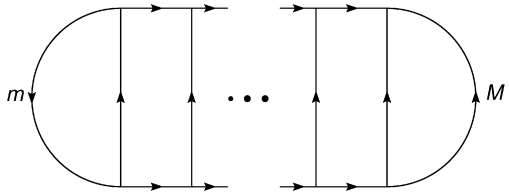

Fig. 11. Two mass scales of vacuum fluctuations of L loops.

while for diagrams of the form (B) we get:

$$
{}_{(2L+1)}F_{2L}\left(\cdots\left|\frac{p^2}{4m^2}\right.\right),
$$

$$
{}_{(2L+1)}F_{2L}\left(\cdots\left|\frac{4m^2}{p^2}\right.\right).
$$

The example (III) of this work corresponds precisely to a diagram of the type (B), in which $L = 4$ and whose solutions are just hypergeometric series of type ${}_9F_8$. Another family of solutions that we can consider are vacuum fluctuations of the type shown in Fig. 11, composed of two energy scales $\{m^2, M^2\}$ and which gives rise to solutions of the form:

$$
{}_{(2L-2)}F_{(2L-3)}\left(\cdots\left|\frac{M^2}{m^2}\right.\right),
$$

$$
{}_{(2L-2)}F_{(2L-3)}\left(\cdots\left|\frac{m^2}{M^2}\right.\right).
$$

In case in which there are three energy scales, the solutions can be expressed in terms of double hypergeometric series. In the calculations performed in the case of one-loop diagrams [6], the solutions are completely described by Appell functions (F_1, F_2, F_3, F_4), one Horn function H_2, and the particular cases S_1 and S_2 of the de Kampé de Fériet function. Nevertheless, for $L > 1$ the number of parameters that characterize the hypergeometrics grows and then it is not possible to describe the solutions with the same functions associated to the 1-loop results and it is necessary to turn to a more general version of the two-variable series $F\,{}^{p:r:u}_{q:s:v}$ or $\bar{F}\,{}^{p:r:u}_{q:s:v}$.

5. Other examples

Although the previously shown examples are sufficient to demonstrate the versatility and power of the method, we want to add briefly other topologies of 2, 3 and 4 external lines. The last two correspond to specific 2-loop topologies to which the method is applicable, and which were not discussed before.

5.1. *Sunset diagram* (Fig. 12)

$$
U = x_1x_2 + x_1x_3 + x_2x_3,
$$

$$
F = x_1x_2x_3p_1^2.
$$

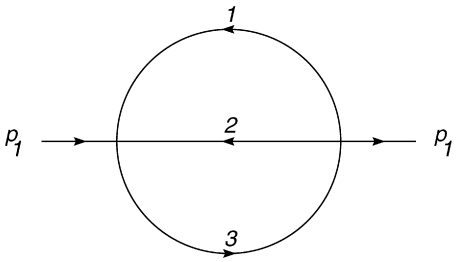

Fig. 12. Sunset diagram.

5.1.1. Massless case ($m_1 = m_2 = m_3 = 0$)

$$G = \frac{(-1)^D}{\prod_{j=1}^3 \Gamma(\nu_j)} \sum_{n_1,\dots,n_4} \Phi_{n_1,\dots,n_4} \frac{(p_1^2)^{n_1}}{\Gamma(\frac{D}{2}+n_1)} \prod_{j=1}^4 \Delta_j, \tag{141}$$

$$\begin{cases} \Delta_1 = \langle \frac{D}{2} + n_1 + n_2 + n_3 + n_4 \rangle, \\ \Delta_2 = \langle \nu_1 + n_1 + n_2 + n_3 \rangle, \\ \Delta_3 = \langle \nu_2 + n_1 + n_2 + n_4 \rangle, \\ \Delta_4 = \langle \nu_3 + n_1 + n_3 + n_4 \rangle. \end{cases} \tag{142}$$

The solution is found immediately, and reads:

$$G = (-1)^D \frac{\Gamma(D/2-\nu_1)\Gamma(D/2-\nu_2)\Gamma(D/2-\nu_3)\Gamma(\nu_1+\nu_2+\nu_3-D)}{\Gamma(\nu_1)\Gamma(\nu_2)\Gamma(\nu_3)\Gamma(3D/2-\nu_1-\nu_2-\nu_3)} \times \left(p_1^2\right)^{D-\nu_1-\nu_2-\nu_3}. \tag{143}$$

5.1.2. Massive case I ($m_1 = m_2 = m$) ($m_3 = 0$)

$$G = \frac{(-1)^D}{\prod_{j=1}^3 \Gamma(\nu_j)} \int_0^\infty d\vec{x} \frac{\exp(-f(-m^2))\exp(-F/U)}{U^{D/2}}. \tag{144}$$

For this particular case U has to be factorized as:

$$U = x_1 x_2 + x_3 f, \qquad f = (x_1 + x_2). \tag{145}$$

$$G = \frac{(-1)^D}{\prod_{j=1}^3 \Gamma(\nu_j)} \sum_{n_1,\dots,n_6} \Phi_{n_1,\dots,n_6} \frac{(-m^2)^{n_1}(p_1^2)^{n_2}}{\Gamma(\frac{D}{2}+n_2)} \frac{\prod_{j=1}^5 \Delta_j}{\Gamma(-n_2-n_4)}, \tag{146}$$

$$\begin{cases} \Delta_1 = \left\langle \frac{D}{2} + n_2 + n_3 + n_4 \right\rangle, \\ \Delta_2 = \langle -n_1 - n_4 + n_5 + n_6 \rangle, \\ \Delta_3 = \langle \nu_1 + n_2 + n_3 + n_5 \rangle, \\ \Delta_4 = \langle \nu_2 + n_2 + n_3 + n_6 \rangle, \\ \Delta_5 = \langle \nu_3 + n_2 + n_4 \rangle. \end{cases} \tag{147}$$

The solutions, in terms of the contributions G_j, are:

$$G\left(\frac{m^2}{p_1^2}\right) = G_1 + G_4 + G_5 + G_6,$$

$$G\left(\frac{p_1^2}{m^2}\right) = G_2. \tag{148}$$

5.1.3. Massive case II $(m_1 = m_2 = m)$ $(m_3 = M)$

$$G = \frac{(-1)^D}{\prod_{j=1}^3 \Gamma(\nu_j)} \int_0^\infty d\vec{x}\, \frac{\exp(-f(-m^2) - x_3(-M^2))\exp(-F/U)}{U^{D/2}}, \tag{149}$$

$$U = x_1x_2 + x_3 f,$$

$$f = (x_1 + x_2), \tag{150}$$

$$G = \frac{(-1)^D}{\prod_{j=1}^3 \Gamma(\nu_j)} \sum_{n_1,\dots,n_7} \Phi_{n_1,\dots,n_7} \frac{(-m^2)^{n_1}(-M^2)^{n_2}(p_1^2)^{n_3}}{\Gamma(\frac{D}{2} + n_3)} \frac{\prod_{j=1}^5 \Delta_j}{\Gamma(-n_1 - n_5)}, \tag{151}$$

$$\begin{cases} \Delta_1 = \langle \frac{D}{2} + n_3 + n_4 + n_5 \rangle, \\ \Delta_2 = \langle -n_1 - n_5 + n_6 + n_7 \rangle, \\ \Delta_3 = \langle \nu_1 + n_3 + n_4 + n_6 \rangle, \\ \Delta_4 = \langle \nu_2 + n_3 + n_4 + n_7 \rangle, \\ \Delta_5 = \langle \nu_3 + n_2 + n_3 + n_5 \rangle. \end{cases} \tag{152}$$

The solutions determine 3 kinematical regions, which we write in terms of the contributions $G_{i,j}$:

$$\begin{aligned} G\left(\frac{4m^2}{p_1^2}, \frac{M^2}{p_1^2}\right) &= G_{1,2} + G_{1,4} + G_{2,5} + G_{2,6} + G_{2,7} + (G_{4,5} = 0) + G_{4,6} + G_{4,7}, \\ G\left(\frac{p_1^2}{4m^2}, \frac{M^2}{4m^2}\right) &= G_{2,3} + G_{3,4}, \\ G\left(\frac{4m^2}{M^2}, \frac{p_1^2}{M^2}\right) &= G_{1,3} + G_{3,5} + G_{3,6} + G_{3,7}. \end{aligned} \tag{153}$$

In each of these cases the contributions $G_{i,j}$ correspond to de Kampé de Fériet functions $(F\,{}^{p:r:u}_{q:s:v})$.

5.2. Massless non-planar double-box diagram (on-shell case) (Fig. 13)

$$U = (x_1 + x_2)(x_5 + x_6) + (x_3 + x_4)(x_5 + x_6) + (x_1 + x_2)(x_3 + x_4),$$

$$F = x_1x_3x_6 s + x_2x_3x_5 u + x_2x_4x_6 t, \tag{154}$$

$$\begin{aligned} G = A \sum_{n_1,\dots,n_{12}} \Phi_{n_1,\dots,n_{12}} &\frac{(s)^{n_1}(u)^{n_2}(t)^{n_3}}{\Gamma(D/2 + n_1 + n_2 + n_3)} \\ &\times \frac{\prod_{j=1}^{10} \Delta_j}{\Gamma(-n_4 - n_6)\Gamma(-n_5 - n_6)\Gamma(-n_4 - n_5)}. \end{aligned} \tag{155}$$

$$A = \frac{(-1)^D}{\prod_{j=1}^6 \Gamma(\nu_j)},$$

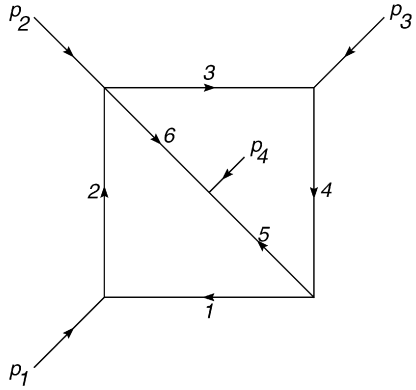

Fig. 13. Labelled non-planar box diagram.

$$\begin{cases} \Delta_1 = \left\langle \frac{D}{2} + n_1 + n_2 + n_3 + n_4 + n_5 + n_6 \right\rangle, \\ \Delta_2 = \langle -n_4 - n_6 + n_7 + n_8 \rangle, \\ \Delta_3 = \langle -n_5 - n_6 + n_9 + n_{10} \rangle, \\ \Delta_4 = \langle -n_4 - n_5 + n_{11} + n_{12} \rangle, \\ \Delta_5 = \langle \nu_1 + n_1 + n_7 \rangle, \\ \Delta_6 = \langle \nu_2 + n_2 + n_3 + n_8 \rangle, \\ \Delta_7 = \langle \nu_3 + n_1 + n_2 + n_9 \rangle, \\ \Delta_8 = \langle \nu_4 + n_3 + n_{10} \rangle, \\ \Delta_9 = \langle \nu_5 + n_2 + n_{11} \rangle, \\ \Delta_{10} = \langle \nu_6 + n_1 + n_3 + n_{12} \rangle. \end{cases}$$

The sets of terms which contribute to the solution are shown as functions of the components $G_{i,j}$ and of the type of two-valued function that represents them:

Set 1: $G_{1,2} + G_{1,12} + G_{2,8} + G_{8,12} \Rightarrow F\left(\left| -\frac{u}{t}, -\frac{s}{t} \right. \right)$,

Set 2: $G_{2,3} + G_{2,9} + G_{3,12} + G_{9,12} \Rightarrow F\left(\left| -\frac{u}{s}, -\frac{t}{s} \right. \right)$,

Set 3: $G_{1,3} + G_{1,9} + G_{3,8} + G_{8,9} \Rightarrow F\left(\left| -\frac{s}{u}, -\frac{t}{u} \right. \right)$,

Set 4: $G_{1,11} + G_{8,11} \Rightarrow \bar{F}\left(\left| -\frac{s}{t}, \frac{t}{u} \right. \right)$,

Set 5: $G_{3,11} + G_{9,11} \Rightarrow \bar{F}\left(\left| -\frac{t}{s}, \frac{s}{u} \right. \right)$,

Set 6: $G_{1,10} + G_{8,10} \Rightarrow \bar{F}\left(\left| -\frac{s}{u}, \frac{u}{t} \right. \right)$,

Set 7: $G_{2,7} \Rightarrow \bar{F}\left(\left| -\frac{u}{t}, \frac{t}{s} \right. \right)$,

Set 8: $G_{7,12} \Rightarrow \bar{F}\left(\left| -\frac{t}{s}, \frac{u}{t} \right. \right)$,

Set 9: $G_{2,10} \Rightarrow \bar{F}\left(\left| -\frac{u}{s}, \frac{s}{t} \right. \right)$,

Set 10: $G_{10,12} \Rightarrow \bar{F}\left(\left| -\frac{s}{t}, \frac{u}{s} \right. \right)$,

Set 11: $G_{3,7} \Rightarrow \bar{F}\left(\left| -\frac{t}{u}, \frac{u}{s} \right. \right)$,

Set 12: $G_{7,9} \Rightarrow \bar{F}\left(\left| -\frac{u}{s}, \frac{t}{u} \right. \right)$,

Set 13: $G_{7,10} \Rightarrow F\left(\left| -\frac{u}{t}, -\frac{u}{s} \right. \right)$,

Set 14: $G_{10,11} \Rightarrow F\left(\left| -\frac{s}{t}, -\frac{s}{u} \right. \right)$,

Set 15: $G_{7,11} \Rightarrow F\left(\left| -\frac{t}{s}, -\frac{t}{u} \right. \right)$.

This example has been solved with the usual NDIM method in Ref. [17]. Nevertheless, it is evident that doing it the way presented here the solutions are found more directly. They are of the type that corresponds to 3 different energy scales, that is two-variable series, although without generating a big number of contributions to the solution, neither redundant sums with unit argument in each one of them. Table 3 allows to visualize more precisely the improvement of our optimization, comparing the solutions obtained without any simplification and with the present method.

5.3. *Four-loop vertex* (Fig. 14)

5.3.1. *A case with 3 energy scales* ($p_1^2 = p_2^2 = 0$) *and* ($m_6 = m$, $m_9 = M$)

$$G = \frac{(-1)^{2D}}{\prod_{j=1}^{9} \Gamma(\nu_j)} \int_0^\infty d\vec{x} \frac{\exp(-x_6(-m^2)) \exp(-x_9(-M^2)) \exp(-F/U)}{U^{D/2}}, \tag{156}$$

Table 3

	Previous NDIM	New NDIM
Possible solutions	6435	66
Relevant solutions	2916	27
Multiplicity (μ)	8	2

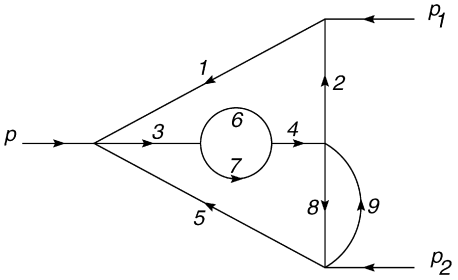

Fig. 14. Labelled four-loop vertex diagram.

$$F = x_1 x_5 f_2 f_5 p^2, \qquad U = f_1 f_4 f_6 + f_1 f_2 f_5 + f_5 f_6, \tag{157}$$

where the functions f_i are given by:

$$\begin{aligned}
f_6 &= x_8 x_9 + x_5 f_2,\\
f_5 &= x_6 x_7 + f_3 f_4,\\
f_4 &= x_6 + x_7,\\
f_3 &= x_3 + x_4,\\
f_2 &= x_8 + x_9,\\
f_1 &= x_1 + x_2,
\end{aligned} \tag{158}$$

$$G = \frac{(-1)^{2D}}{\prod_{j=1}^{9}\Gamma(\nu_j)} \sum_{n_1,\ldots,n_{18}} \Phi_{n_1,\ldots,n_{18}} \frac{(-m^2)^{n_1}(-M^2)^{n_2}(p^2)^{n_3}}{\Gamma(\frac{D}{2}+n_3)}\, \Omega_{\{n\}} \prod_{j=1}^{16} \Delta_j, \tag{159}$$

where the factor $\Omega_{\{n\}}$ is:

$$\Omega_{\{n\}} = \frac{1}{\Gamma(-n_4-n_5)\Gamma(-n_3-n_5-n_6)\Gamma(-n_4-n_6)\Gamma(-n_3-n_5-n_{12})\Gamma(-n_{10})\Gamma(-n_4-n_{10})}, \tag{160}$$

$$\begin{cases}
\Delta_1 = \langle \frac{D}{2}+n_3+n_4+n_5+n_6\rangle, & \Delta_9 = \langle \nu_2+n_8\rangle,\\
\Delta_2 = \langle -n_4-n_5+n_7+n_8\rangle, & \Delta_{10} = \langle \nu_3+n_{15}\rangle,\\
\Delta_3 = \langle -n_3-n_5-n_6+n_9+n_{10}\rangle, & \Delta_{11} = \langle \nu_4+n_{16}\rangle,\\
\Delta_4 = \langle -n_4-n_6+n_{11}+n_{12}\rangle, & \Delta_{12} = \langle \nu_5+n_3+n_{12}\rangle,\\
\Delta_5 = \langle -n_3-n_5-n_{12}+n_{13}+n_{14}\rangle, & \Delta_{13} = \langle \nu_6+n_1+n_9+n_{17}\rangle,\\
\Delta_6 = \langle -n_{10}+n_{15}+n_{16}\rangle, & \Delta_{14} = \langle \nu_7+n_9+n_{18}\rangle,\\
\Delta_7 = \langle -n_4-n_{10}+n_{17}+n_{18}\rangle, & \Delta_{15} = \langle \nu_8+n_{11}+n_{13}\rangle,\\
\Delta_8 = \langle \nu_1+n_3+n_7\rangle, & \Delta_{16} = \langle \nu_9+n_2+n_{11}+n_{14}\rangle.
\end{cases}$$

The sets of solutions are given by the following equations in terms of the contributions $G_{i,j}$.

Set 1: $G_{1,2} + G_{1,5} + G_{1,13} + G_{2,4} + G_{2,18} + (G_{4,5} = 0) + G_{4,13} + G_{5,18} + G_{13,18} \Rightarrow F\left(\left| \frac{m^2}{p^2}, -\frac{M^2}{p^2} \right.\right)$,

Set 2: $G_{1,3} + G_{3,4} + G_{3,18} \Rightarrow F\left(\left| \frac{m^2}{M^2}, -\frac{p^2}{M^2} \right.\right)$,

Set 3: $G_{2,3} + G_{3,5} + G_{3,13} \Rightarrow F\left(\left| \frac{M^2}{m^2}, \frac{p^2}{m^2} \right.\right)$,

Set 4: $G_{7,9} + G_{9,12} \Rightarrow F\left(\left| \frac{M^2}{m^2}, -\frac{M^2}{p^2} \right.\right)$,

Set 5: $G_{7,11} + (G_{11,12} = 0) \Rightarrow F\left(\left| \frac{m^2}{M^2}, \frac{m^2}{p^2} \right.\right)$,

Set 6: $G_{9,11} \Rightarrow F\left(\left| \frac{p^2}{m^2}, -\frac{p^2}{M^2} \right.\right)$,

Set 7: $G_{1,11} + G_{4,11} \Rightarrow \bar{F}\left(\left| \frac{m^2}{p^2}, \frac{p^2}{M^2} \right.\right)$,

Set 8: $G_{11,18} \Rightarrow \bar{F}\left(\left| -\frac{p^2}{M^2}, -\frac{m^2}{p^2} \right.\right)$,

Set 9: $G_{2,9} + G_{5,9} \Rightarrow \bar{F}\left(\quad \left| -\frac{M^2}{p^2}, -\frac{p^2}{m^2} \right. \right)$,

Set 10: $G_{9,13} \Rightarrow \bar{F}\left(\quad \left| \frac{p^2}{m^2}, \frac{M^2}{p^2} \right. \right)$,

Set 11: $G_{1,7} + G_{1,12} + G_{4,7} + G_{4,12} \Rightarrow \bar{F}\left(\quad \left| \frac{m^2}{M^2}, \frac{M^2}{p^2} \right. \right)$,

Set 12: $G_{7,18} + G_{12,18} \Rightarrow \bar{F}\left(\quad \left| -\frac{M^2}{p^2}, -\frac{m^2}{M^2} \right. \right)$,

Set 13: $G_{3,9} \Rightarrow \bar{F}\left(\quad \left| -\frac{p^2}{M^2}, -\frac{M^2}{m^2} \right. \right)$,

Set 14: $G_{2,7} + G_{2,12} + G_{5,7} + G_{5,12} \Rightarrow \bar{F}\left(\quad \left| \frac{M^2}{m^2}, -\frac{m^2}{p^2} \right. \right)$,

Set 15: $G_{7,13} + G_{12,13} \Rightarrow \bar{F}\left(\quad \left| \frac{m^2}{p^2}, -\frac{M^2}{m^2} \right. \right)$,

Set 16: $G_{3,11} \Rightarrow \bar{F}\left(\quad \left| \frac{p^2}{m^2}, -\frac{m^2}{M^2} \right. \right)$.

In this example the fact that $(M^2 > m^2)$ or vice versa leaves out automatically sets of solutions, since only one of these conditions can appear in the same topology.

6. Conclusions

The integration method here presented is a powerful tool for solving Feynman integrals with arbitrary exponents in the propagators. Its main characteristics resides in its simplicity in finding the solution of diagrams, even in the evaluation of L-loop diagrams. This technique, which can be more appropriately called integration by fractional expansion, is clearly an important competitor to other Feynman diagram evaluation methods. In spite of its generality, we have found that the technique is adequately applicable to certain types of graphs, obtaining solutions which we call optimal, in the sense that they are algebraically manageable, and whose complexity does not depend on the number of loops L of the diagram. Although this method can be applied to any diagram, the complexity of the solutions in the more general cases has a high dependence on L, which implies a large number of terms as well as a high multiplicity μ of the resulting series expansions, which makes the analysis of the solution highly nontrivial. Imposing to evaluate only topologies whose solutions can be represented as series in which the variables are expressed as ratios between the different energy scales of the diagram, determines that the multiplicity of each of them fulfills the relation $\mu = (n - 1)$, where n is the number of different energy scales in the diagram. This is the restriction that allowed us to find that the method here proposed is applicable in a natural way to certain L-loop class of diagrams, which in the massless case happen to be solvable loop by loop. Using this condition it becomes possible, depending on the number of energy scales present in this class of topologies, obtain solutions as expansions in multivalued series. Nevertheless, we have considered adequate to evaluate topologies whose solutions could be expressed at most in terms of two-variable series, because hypergeometric series of this type have been amply treated in the literature. The advantages of this integration method can be summarized in the following:

- For the family of L loop graphs, reducible recursively loop-by-loop, the application of the technique makes possible to find the solution considering all loops simultaneously, through its Schwinger parametric representation.
- The integration method allows to extend in a simple manner the solutions to cases in which different mass scales are considered in the graph.
- It is possible to apply the integration method to certain 3 and 4 external line topologies, and generalize it to L loops making one-loop insertions in the propagators. In general the application of this technique can be extended to more external lines, but the solutions are series with $\mu > 2$, and therefore have not been considered in this work.
- Independently of the number of loops, in topologies of the loop by loop reducible type, the multiplicity μ of the hypergeometric series solution does not have any dependence on the number of loops L, and only depends on the number of different energy scales that characterize the graph. For topologies that are not in the class reducible loop-by-loop, except for the special cases described previously, the multiplicity grows when L increases. This fact makes this type of topologies not optimal for the application of the method, because the complexity of the solutions grows very quickly with L. We can estimate this growth in terms of the contributions that the solution contains, using the following expression:

$$\text{Number of contributions of the solution} \sim \frac{(\mu(L)+\delta)!}{\delta!(\mu(L))!}.$$

A significant fact is that the method allows to easily add masses to any type of topologies. In general for generic diagrams we have been able to conclude that:

- If we add M different mass scales, the multiplicity of the series expressions that are part of the solution grows in M units.
- In most cases if we add masses to propagators belonging to l different loops, the masses have to be considered different, even if they have the same value, and the multiplicity increases in l units.
- The conjunction of the previous premises implies that if one associates M equal masses to the propagators of a loop, the multiplicity of the series solution only increases in one unit.

Appendix A. Mathematical formalism of NDIM

In Section 2.2 the technique was introduced, and also its origins starting from the identity associated to the loop integral parametrization and known as Schwinger's parametrization:

$$\frac{1}{A^{\beta}} = \frac{1}{\Gamma(\beta)} \int_0^{\infty} dx\, x^{\beta-1} \exp(-Ax), \tag{A.1}$$

and furthermore the equivalence between the integral symbol and a delta Kronecker (13) was shown starting from Eq. (A.1):

$$\int dx\, x^{\beta+n-1} \equiv \frac{\Gamma(\beta)\Gamma(n+1)}{(-1)^n} \delta_{\beta+n,0}. \tag{A.2}$$

For simplicity we have eliminated the limits of the integral, since this identity has validity only in the context of the expansion of the integrand in (A.1). This expression is crucial for the devel-

opment of the method NDIM, since in the evaluation of Feynman diagrams the corresponding Schwinger parametric representation is a generalized structure of the expression (A.1).

A.1. Some properties

In order to study some of the properties of (A.2), it is convenient to introduce a useful notation for helping us to formalize the mechanism of the technique NDIM. Thus:

$$\int dx\, x^{\nu_1+\nu_2-1} \equiv \langle \nu_1+\nu_2 \rangle, \tag{A.3}$$

where ν_1 and ν_2 are indexes that can assume arbitrary values.

A.1.1. Property I. Commutativity of indexes

We can write (A.3) explicitly in 2 possible forms, according to formula (A.2), and then:

$$\langle \nu_1+\nu_2 \rangle = \begin{cases} \frac{\Gamma(\nu_1)\Gamma(\nu_2+1)}{(-1)^{\nu_2}}\delta_{\nu_1+\nu_2,0}, \\ \frac{\Gamma(\nu_2)\Gamma(\nu_1+1)}{(-1)^{\nu_1}}\delta_{\nu_1+\nu_2,0}. \end{cases} \tag{A.4}$$

Starting from (A.1) it is possible to show the equivalence of both forms in (A.4), and for this purpose it is enough to expand the exponential of the integrand and replace $\langle\cdot\rangle$ for this case.

Let us consider the following integral representation:

$$\frac{1}{A^{\nu_1}} = \frac{1}{\Gamma(\nu_1)} \int_0^\infty dx\, x^{\nu_1-1} \exp(-Ax), \tag{A.5}$$

which in terms of series, in the sense proposed (A.3), turns out to be:

$$\frac{1}{A^{\nu_1}} = \frac{1}{\Gamma(\nu_1)} \sum_{\nu_2} \frac{(-1)^{\nu_2}}{\Gamma(\nu_2+1)} A^{\nu_2} \langle \nu_1+\nu_2 \rangle. \tag{A.6}$$

Selecting now $\langle \nu_1+\nu_2 \rangle = \frac{\Gamma(\nu_1)\Gamma(\nu_2+1)}{(-1)^{\nu_2}}\delta_{\nu_1+\nu_2,0}$, we directly obtain the equality in (A.5). Analogously selecting $\langle \nu_1+\nu_2 \rangle = \frac{\Gamma(\nu_2)\Gamma(\nu_1+1)}{(-1)^{\nu_1}}\delta_{\nu_1+\nu_2,0}$ and using afterwards the identity:

$$\frac{\Gamma(y)}{\Gamma(y-z)} = (-1)^{-z} \frac{\Gamma(1+z-y)}{\Gamma(1-y)}, \tag{A.7}$$

with $y=\nu_1$ and $z=2\nu_1$, the equality (A.5) is obtained once again, and therefore the equivalence between both forms of writing $\langle \nu_1+\nu_2 \rangle$ is quickly established.

Another form of writing (A.3), which is quite useful for simplifying terms that contain the factor:

$$\frac{1}{\Gamma(m+1)}, \tag{A.8}$$

where m is an arbitrary index, is the following:

$$\langle \nu_1+\nu_2 \rangle = \langle \nu_1+\nu_2-m+m \rangle = \langle -m+m \rangle = \frac{\Gamma(-m)\Gamma(m+1)}{(-1)^m}\delta_{\nu_1+\nu_2,0}. \tag{A.9}$$

Notice that we have made explicit use of the Kronecker delta in order to simplify the parenthesis $\langle\cdot\rangle$, and since this is in the context of expansions, the Kronecker delta remains as an indication of the constraints between the indexes ν_1 and ν_2.

A.1.2. Property ll. Multiregion expansion

Consider the binomial expression:

$$(A_1 + A_2)^{\pm\nu}, \tag{A.10}$$

where the quantities A_1, A_2 and ν, can take arbitrary values. In this case there are two limits or possible regions with respect to the expansion: the region where $(A_1 > A_2)$ and the region where $(A_1 < A_2)$. These expansions are respectively:

1. Region $(A_1 > A_2)$

$$(A_1 + A_2)^{\pm\nu} = A_1^{\pm\nu} \sum_{n=0}^{\infty} \frac{(\mp\nu)_n}{\Gamma(n+1)} \left(-\frac{A_2}{A_1}\right)^n. \tag{A.11}$$

2. Region $(A_1 < A_2)$

$$(A_1 + A_2)^{\pm\nu} = A_2^{\pm\nu} \sum_{n=0}^{\infty} \frac{(\mp\nu)_n}{\Gamma(n+1)} \left(-\frac{A_1}{A_2}\right)^n. \tag{A.12}$$

The factor $(\nu)_n$ is called Pochhammer symbol and is defined as:

$$(\nu)_n = \frac{\Gamma(\nu+n)}{\Gamma(\nu)}. \tag{A.13}$$

We have thus obtained separate expansions in the two possible limits. Nevertheless, it is possible to express both results using a single series that contains both limiting regions. In this sense we can say that this type of expansion corresponds to a multiregion series representation of the binomial (A.10), through the use of the integral representation of the denominator indicated in (A.1). Then we have:

$$(A_1 + A_2)^{\pm\nu} = \frac{1}{\Gamma(\mp\nu)} \int_0^{\infty} dx\, x^{\mp\nu-1} \exp(-xA_1) \exp(-xA_2), \tag{A.14}$$

and the exponentials are expanded separately, with the result:

$$(A_1 + A_2)^{\pm\nu} = \frac{1}{\Gamma(\mp\nu)} \sum_{n_1} \sum_{n_2} \frac{(-1)^{n_1+n_2}}{\Gamma(n_1+1)\Gamma(n_2+1)} A_1^{n_1} A_2^{n_2} \int dx\, x^{\mp\nu+n_1+n_2-1}. \tag{A.15}$$

Making use of the identity (A.3) we get the multiregion binomial expansion:

$$(A_1 + A_2)^{\pm\nu} = \frac{1}{\Gamma(\mp\nu)} \sum_{n_1} \sum_{n_2} \frac{(-1)^{n_1+n_2}}{\Gamma(n_1+1)\Gamma(n_2+1)} A_1^{n_1} A_2^{n_2} \langle \mp\nu + n_1 + n_2 \rangle, \tag{A.16}$$

where the parenthesis $\langle\cdot\rangle$, according to property (A.4), can be expressed this time in three different ways, although in each one of them we will have the same Kronecker delta which eliminates one of the two sums that are present:

$$\langle \mp\nu + n_1 + n_2 \rangle = \begin{cases} \frac{\Gamma(\mp\nu+n_1)\Gamma(n_2+1)}{(-1)^{n_2}} \delta_{\mp\nu+n_1+n_2,0}, \\ \frac{\Gamma(\mp\nu+n_2)\Gamma(n_1+1)}{(-1)^{n_1}} \delta_{\mp\nu+n_1+n_2,0}, \\ \frac{\Gamma(n_2+n_1)\Gamma(\mp\nu+1)}{(-1)^{\mp\nu}} \delta_{\mp\nu+n_1+n_2,0}. \end{cases} \tag{A.17}$$

On the other hand, the number of possible forms of summing (A.16) using for this purpose the Kronecker delta, can be found evaluating the combinatorics $C^{\text{Sums}}_{\text{Deltas}}$, which in this case is $C^2_1 = 2$. Let us see what happens if one sums with respect to a particular index:

1. *Sum respect to* n_2

Using for this case the following equality:

$$\langle \mp\nu + n_1 + n_2 \rangle = \frac{\Gamma(\mp\nu + n_1)\Gamma(n_2 + 1)}{(-1)^{n_2}} \delta_{\mp\nu+n_1+n_2,0}, \tag{A.18}$$

and then replacing in (A.16), we get:

$$(A_1 + A_2)^{\pm\nu} = \frac{1}{\Gamma(\mp\nu)} \sum_{n_1} (-1)^{n_1} \frac{\Gamma(\mp\nu + n_1)}{\Gamma(n_1 + 1)} A_1^{n_1} A_2^{\mp\nu - n_1}, \tag{A.19}$$

or equivalently:

$$(A_1 + A_2)^{\pm\nu} = A_2^{\pm\nu} \sum_{n_1=0}^{\infty} \frac{(\mp\nu)_{n_1}}{\Gamma(n_1 + 1)} \left(-\frac{A_1}{A_2}\right)^{n_1}, \tag{A.20}$$

which gives the expression associated to the region $(A_1 < A_2)$, obtained previously in (A.12).

2. *Sum respect to* n_1

Analogously, we now use the identity:

$$\langle \mp\nu + n_1 + n_2 \rangle = \frac{\Gamma(\mp\nu + n_2)\Gamma(n_1 + 1)}{(-1)^{n_1}} \delta_{\mp\nu+n_1+n_2,0}, \tag{A.21}$$

and replacing in (A.16), one gets:

$$(A_1 + A_2)^{\pm\nu} = A_1^{\pm\nu} \sum_{n_2=0}^{\infty} \frac{(\mp\nu)_{n_2}}{\Gamma(n_2 + 1)} \left(-\frac{A_2}{A_1}\right)^{n_2}, \tag{A.22}$$

an expression that was already found in (A.11), and valid in the region $(A_1 > A_2)$.

The fundamental idea that has been exposed in the previous demonstration is that using the definition (A.2) one can do a binomial expansion that differs from the conventional expansion, in the sense that one obtains an expression where all the possible limits of the binomial are included simultaneously.

A.2. Multiregion expansion of a multinomial

The previous discussion can be generalized to the multiregion expansion of a multinomial of n_l terms:

$$(A_1 + \cdots + A_l)^{\pm\nu} = \frac{1}{\Gamma(\mp\nu)} \sum_{n_1} \cdots \sum_{n_l} \Phi_{n_1,\ldots,n_l}\, A_1^{n_1} \cdots A_l^{n_l} \langle \mp\nu + n_1 + \cdots + n_l \rangle, \tag{A.23}$$

where for simplicity we have defined the following notation:

$$\Phi_{n_1,\ldots,n_l} = (-1)^{n_1+\cdots+n_l} \frac{1}{\Gamma(n_1+1)\cdots\Gamma(n_l+1)}. \tag{A.24}$$

The number of expansions that can be obtained starting from (A.23) is given at most by all the possible forms of evaluating some of the sums, using for this the Kronecker delta generated by the same expansion, that is $C_1^{n_l} = n_l$ possible forms. More generally, a function expressed as a multiregion expansion through σ sums and δ Kronecker deltas, can be evaluated at most in:

$$C_\delta^\sigma = \frac{\sigma!}{\delta!(\sigma-\delta)!} \tag{A.25}$$

possible forms, each one of them expressed in terms of series of multiplicity $\mu = (\sigma - \delta)$. All the resulting series are representations with respect to the ratios between the terms of the multinomial, and all of them correspond to multivariable generalizations of the hypergeometric function.

Appendix B. Negative dimension D?

The original name of the integration method here presented, NDIM (negative dimension integration method), comes from applying the expansion and subsequent association, integral $\Leftrightarrow$ Kronecker delta, over the Gaussian integral in D dimensions:

$$\int \frac{d^D k}{i\pi^{\frac{D}{2}}} \exp\bigl(\alpha k^2\bigr), \tag{B.1}$$

where k corresponds to a 4-momentum and α is an arbitrary parameter. This is a typical integral that appears upon using Schwinger's parametrization and after using the completion of squares procedure of the loop momenta. Starting from this equation it is possible to deduce in a similar way to Eq. (13) the following identity [5]:

$$\int \frac{d^D k}{i\pi^{\frac{D}{2}}} \bigl(k^2\bigr)^n = n!\delta_{n+\frac{D}{2},0}. \tag{B.2}$$

Since this is in fact a Taylor expansion, we assume that $n \geqslant 0$, and therefore the constraint associated to the Kronecker delta in (B.2) requires that $\frac{D}{2} \leqslant 0$, that is, la dimension has to be negative, which is then the origin of the name of this integration technique. Nevertheless, there can appear reasonable doubts with respect to some concepts that the NDIM uses in its original approach.

It is entirely possible for D to be a negative integer considering that the Feynman integrals are analytic functions in D arbitrary dimensions, but rigorously what is wanted is to solve the loop integrals in the limit $D \to +4$ and not in the limit $D \to -4$. The inconsistency is even more clear if the dimensional regularization prescription is used, and the dimension D now includes a non-integer piece, the dimensional regulator ϵ, which cannot be associated to the sum index n in (B.2).

Such inconsistencies could be resolved if the expansion of the exponential could be written as:

$$\exp(x) = \lim_{\xi\to 0} \sum_{m=-\infty+\xi}^{\infty+\xi} \frac{x^m}{\Gamma(m+1)} \quad \text{such that } \left.\frac{d^m \exp(x)}{dx^m}\right|_{x=0} = 1, \tag{B.3}$$

where $|\xi| < 1$ and m is an index that increases in one unit steps. Such an expansion is possible, but for this purpose it is necessary to resort to the area of calculus called fractional calculus [23–25], through which it can be shown that both the derivative and the integration operators can be represented in terms of a unique operator, and in second term shows that the analytical continuation in the operator order can in fact be done, and can be fractional and even complex. This is very useful in order to justify the validity of the NDIM integration technique, and therefore it is necessary to review some concepts for understanding this type of calculus.

B.1. Preliminaries: The fractional expansion of the exponential function

We are interested in knowing the nature of the expansion that is performed in the exponential function in (B.1), since due to the arguments mentioned before it should not really correspond to a Taylor expansion.

In order to provide a more rigorous basis for Eq. (B.3), it becomes necessary to define the integration and derivative operators in a generalized form. In fractional calculus is possible to define the fractional integral of order α as follows:

$${}_cD_x^{-\alpha} f(x) = \frac{1}{\Gamma(\alpha)} \int_c^x dt \frac{f(t)}{(x-t)^{1-\alpha}}, \tag{B.4}$$

where $c \in \mathbb{R}$ and α is an arbitrary quantity. For the particular case in which $c = 0$ in (B.4), we get the so-called Riemann–Liouville fractional integral:

$${}_0D_x^{-\alpha} f(x) = \frac{1}{\Gamma(\alpha)} \int_0^x dt \frac{f(t)}{(x-t)^{1-\alpha}}. \tag{B.5}$$

Another version of the fractional integral can be obtained making $c = -\infty$, which is called Liouville fractional integral:

$${}_{-\infty}D_x^{-\alpha} f(x) = \frac{1}{\Gamma(\alpha)} \int_{-\infty}^x dt \frac{f(t)}{(x-t)^{1-\alpha}}. \tag{B.6}$$

This last version of the fractional integral will be used in this work in order to justify more rigorously the integration method of Feynman diagrams here presented. Certainly this would be incomplete if we do not define also the fractional derivative (in the Liouville version). For an order α which fulfills that $(m-1) < \alpha \leqslant m$, with $m \in \mathbb{N}$, the fractional derivative is defined by the expression ${}_{-\infty}D_x^{\alpha} f(x) = \frac{d^m}{dx^m}[{}_{-\infty}D_x^{m-\alpha} f(x)]$, or in operational terms:

$${}_{-\infty}D_x^{\alpha} f(x) = \begin{cases} \frac{1}{\Gamma(m-\alpha)} \frac{d^m}{dx^m} \int_{-\infty}^x dt \frac{f(t)}{(x-t)^{1+\alpha-m}}, & (m-1) < \alpha < m, \\ \frac{d^m}{dx^m} f(x), & \alpha = m. \end{cases} \tag{B.7}$$

We are particularly interested in the Liouville integro-differential operator, so for simplifying the notation let us define ${}_{-\infty}D_x^\alpha = D_x^\alpha$, where we can have ($\alpha < 0$), which is an integral, or ($\alpha > 0$), a derivative.

A property that makes this version of the fractional operator particularly interesting is the effect that it has over the exponential function, and which in practice is an extension of what is done by integrals and derivatives of integer order (conventional calculus) over this function:

$$D_x^\alpha\big[\exp(\beta x)\big] = \begin{cases} \beta^{-\alpha}\exp(\beta x) & \alpha < 0 \text{ (integration of order } \alpha), \\ \beta^{\alpha}\exp(\beta x) & \alpha > 0 \text{ (derivation of order } \alpha). \end{cases} \tag{B.8}$$

This expression can be easily proved using Eqs. (B.6) and (B.7).

B.2. Taylor and Taylor–Riemann series. The fractional expansion of diagram G

Particular interest has the series representation of the exponential function, since it is the only function over which the expansions in the Schwinger parameter integral are done, either because it appears explicitly in the integrand, or because it is used implicitly in order to do the multiregion expansions of the multinomials present in the problem. When the expansions in the integral of the parametric integral are done, we automatically assume that this is a Taylor series. Nevertheless, what is really done implicitly is a Taylor–Riemann expansion of the exponential, which reads:

$$\exp(x) = \sum_{n=-\infty}^{\infty} D_x^{n+\xi}\big[\exp(x)\big]\big|_{x=0}\frac{x^{n+\xi}}{\Gamma(n+\xi+1)}. \tag{B.9}$$

The parameter ξ is arbitrary and fulfills the condition $0 \leqslant |\xi| < 1$. Notice that taking $\xi \to 0$ the Taylor series for the exponential is obtained. Moreover, since $D_x^{n+\xi}[\exp(x)]|_{x=0} = 1$, according to formula (B.8), one gets:

$$\exp(x) = \sum_{n=-\infty}^{\infty} \frac{x^{n+\xi}}{\Gamma(n+\xi+1)}. \tag{B.10}$$

If we make now the change of variables $m = n + \xi$, we can rewrite the previous expansion as:

$$\exp(x) = \sum_{m=-\infty+\xi}^{\infty+\xi} \frac{x^{m}}{\Gamma(m+1)}, \tag{B.11}$$

which looks like the conventional Taylor series expansion of the exponential, with the difference that the index of the sum has been analytically continued to negative and fractional values. This justifies that both D and the propagator powers $\{\nu_1, \ldots, \nu_N\}$ do not change its nature due to some analytical continuation required by the Kronecker deltas generated in the process, but rather are the expansion indexes the ones that can acquire arbitrary values, including negative and fractional. But moreover it justifies the presence of gamma functions in the multiregion expansion of the diagram, both in the numerator and denominator, which having the form $\Gamma(-n)$, where n is an index associated to a sum, give a multiregion expansion not necessarily infinite or vanishing.

After having said that, it is still necessary to justify what refers to the integration method, since they correspond to hypergeometric series whose summation indexes are positive integers. This can be explained by saying that for applying the integration method NDIM an analytical continuation of the summation indexes has to be done, or equivalently the exponentials are expanded in Taylor–Riemann series, using the expression (B.11). In practical terms it is enough to

assume a fractional arbitrary parameter ξ associated to the indexes of all the sums, and at the end of the integration process, when each contribution to the solution is determined, evaluate the limit:

$$\lim_{\xi\to 0}\sum_{m=-\infty+\xi}^{\infty+\xi} \Rightarrow \sum_{m=0}^{\infty}, \tag{B.12}$$

which naturally happens since all the solutions that are obtained have the factor $1/\Gamma(m+1+\xi)$, and in the limit $\xi\to 0$ we have that:

$$\lim_{\xi\to 0}\frac{1}{\Gamma(m+1+\xi)} = \begin{cases} \frac{1}{m!}, & \text{para } m \geqslant 0, \\ 0, & \text{para } m < 0. \end{cases} \tag{B.13}$$

Therefore, strictly speaking we should write the multiregion expansion (21) of a generic diagram G in the following form:

$$G = (-1)^{\frac{LD}{2}} \lim_{\xi_1,\ldots,\xi_\sigma\to 0} \sum_{n_1=-\infty+\xi_1}^{\infty+\xi_1} \cdots \sum_{n_\sigma=-\infty+\xi_\sigma}^{\infty+\xi_\sigma} \Phi_{n_1,\ldots,n_\sigma} \prod_{j=1}^{P} \left(Q_j^2\right)^{n_j} \prod_{j=P+1}^{P+M} \left(-m_j^2\right)^{n_j} \times \prod_{j=1}^{N} \frac{\langle \nu_j + \alpha_j\rangle}{\Gamma(\nu_j)} \prod_{j=1}^{K} \frac{\langle \beta_j + \gamma_j\rangle}{\Gamma(\beta_j)}. \tag{B.14}$$

Operationally NDIM does not consider the presence of the fractional part ξ in the summation index nor its extension to negative values. Nevertheless, the analytic continuation of the summation indexes and the evaluation of the limit at the end of the process, are inherent to the process and justify why it works. A confusion might arise from the similarity of the Taylor series expansion of the exponential and its Taylor–Riemann expansion (Eq. (B.11)), something that explains why both versions of the expansion give the same result, which in turn shows that there is a conceptual but not operational difference. Thus it would be more appropriate to call the method integration by fractional expansion (IBFE) instead of NDIM.

Appendix C. Hypergeometric functions of 1 and 2 variables

In this work we have developed the evaluation of loop integrals of certain class of diagrams with arbitrary L. All the found solutions have been presented in terms of hypergeometric series of 1 or 2 variables, which correspond in a natural way to an serie representation with respect to the ratio between the energy scales associated to the graph. The purpose of this appendix is precisely to provide the necessary information about the hypergeometric functions [26–29] and especially with respect to their convergence properties.

C.1. Definition of the generalized hypergeometric function

In those cases in which the solutions contain two energy scales the series representations are expressed in terms of generalized hypergeometric functions:

$${}_qF_{q-1}(a_1,\ldots,a_q;b_1,\ldots,b_{q-1};z) \equiv {}_qF_{q-1}\left(\left.\begin{matrix}\{a\}\\ \{b\}\end{matrix}\right| z\right) = \sum_{k=0}\frac{(a_1)_k\cdots(a_q)_k}{(b_1)_k\cdots(b_{q-1})_k}\frac{z^k}{k!}, \tag{C.1}$$

where the factors $(\alpha)_k$ are called Pochhammer symbols, defined as:

$$(\alpha)_k = \frac{\Gamma(\alpha + k)}{\Gamma(\alpha)}. \tag{C.2}$$

The convergence conditions for these series are given according to the magnitude of the argument:

1. If $|z| < 1$ the series converges absolutely. The variable z represents the ratio between energy scales of the topology.
2. If $z = 1$, the necessary requirement for the convergence of the series is that $\mathrm{Re}(\omega) > 0$, where ω is called parametric excess and is given by:

$$\omega = \sum_{j=0}^{q} b_j - \sum_{j=0}^{q+1} a_j. \tag{C.3}$$

For the convergence when $z = -1$ it is sufficient that $\mathrm{Re}(\omega) > -1$.

C.2. Some identities of the Pochhammer symbols

The following identities are useful when building the hypergeometric function from the contributions that in turn are obtained from the multiregion expansion of an arbitrary diagram G. The Pochhammer symbols are defined as follows:

$$(a)_n = \begin{cases} \prod_{j=0}^{n-1}(a+j) & \text{if } n > 0, \\ 1 & \text{if } n = 0, \\ \prod_{j=1}^{n} \frac{1}{(a-j)} & \text{if } n < 0 \quad \text{and} \quad a \notin \{0, -1, -2, \ldots, -n\}. \end{cases} \tag{C.4}$$

Nevertheless, the series that are the result of applying the NDIM to Feynman integrals will always contain factors of the type $\Gamma(a \pm n)$ and $\Gamma(a \pm 2n)$. In these cases it is convenient to use the following formulae for finding the hypergeometric representations:

$$(a)_n = \frac{\Gamma(a+n)}{\Gamma(a)}, \tag{C.5}$$

$$(a)_{-n} = \frac{\Gamma(a-n)}{\Gamma(a)} = \frac{(-1)^n}{(1-a)_n}, \tag{C.6}$$

$$(a)_{\pm 2n} = \frac{\Gamma(a \pm 2n)}{\Gamma(a)} = 4^n \left(\frac{a}{2}\right)_{\pm n} \left(\frac{a}{2} + \frac{1}{2}\right)_{\pm n}. \tag{C.7}$$

C.3. Two-variable hypergeometric functions

In this part of the appendix we describe the functions which are useful for representing those cases that consider three different energy scales, in the general case $L > 1$. Such functions correspond to the de Kampé de Fériet generalized double hypergeometric function $F\,{}^{p:r:u}_{q:s:v}$ and the generalized hypergeometric $\bar{F}\,{}^{p:r:u}_{q:s:v}$. The first is defined as:

$$
\begin{aligned}
&F\,{}^{p:r:u}_{q:s:v}\left(\begin{matrix}\alpha_1,\ldots,\alpha_p & a_1,\ldots,a_r & c_1,\ldots,c_u\\ \beta_1,\ldots,\beta_q & b_1,\ldots,b_s & d_1,\ldots,d_v\end{matrix}\,\middle|\,x,y\right)\\
&\quad= F\,{}^{p:r:u}_{q:s:v}\left(\begin{matrix}\{\alpha\} & \{a\} & \{c\}\\ \{\beta\} & \{b\} & \{d\}\end{matrix}\,\middle|\,x,y\right)\\
&\quad= \sum_{n,m}\frac{\prod_{j=1}^{p}(\alpha_j)_{n+m}\prod_{j=1}^{r}(a_j)_n\prod_{j=1}^{u}(c_j)_m}{\prod_{j=1}^{q}(\beta_j)_{n+m}\prod_{j=1}^{s}(b_j)_n\prod_{j=1}^{v}(d_j)_m}\frac{x^n}{n!}\frac{y^m}{m!},
\end{aligned}
\tag{C.8}
$$

where the convergence of the double series requires that the following relation between the indexes is fulfilled:

$$p+r\leqslant q+s+1, \tag{C.9}$$

$$p+u\leqslant q+v+1, \tag{C.10}$$

and also that the arguments fulfill the condition:

$$|x|^{\frac{1}{(p-q)}}+|y|^{\frac{1}{(p-q)}}<1, \qquad \text{for the case in which } (p>q), \tag{C.11}$$

$$\max\{|x|,|y|\}<1, \qquad \text{in the case } (p\leqslant q). \tag{C.12}$$

For the other series that occurs frequently we have the following definition:

$$
\begin{aligned}
&\bar{F}\,{}^{p:r:u}_{q:s:v}\left(\begin{matrix}\alpha_1,\ldots,\alpha_p & a_1,\ldots,a_r & c_1,\ldots,c_u\\ \beta_1,\ldots,\beta_q & b_1,\ldots,b_s & d_1,\ldots,d_v\end{matrix}\,\middle|\,x,y\right)\\
&\quad= \bar{F}\,{}^{p:r:u}_{q:s:v}\left(\begin{matrix}\{\alpha\} & \{a\} & \{c\}\\ \{\beta\} & \{b\} & \{d\}\end{matrix}\,\middle|\,x,y\right)\\
&\quad= \sum_{n,m}\frac{\prod_{j=1}^{p}(\alpha_j)_{n-m}\prod_{j=1}^{r}(a_j)_n\prod_{j=1}^{u}(c_j)_m}{\prod_{j=1}^{q}(\beta_j)_{n-m}\prod_{j=1}^{s}(b_j)_n\prod_{j=1}^{v}(d_j)_m}\frac{x^n}{n!}\frac{y^m}{m!},
\end{aligned}
$$

where the convergence of the double series requires that the following relations between the indexes are satisfied:

$$p+r\leqslant q+s+1, \tag{C.13}$$

$$q+u\leqslant p+v+1. \tag{C.14}$$

All solutions obtained with the technique of integration NDIM fulfill the previous condition in the sum indexes. The conditions of convergence of arguments may be worked out using Horns general theory of convergence [30].

References

[1] V.A. Smirnov, Evaluating Feynman Integrals, Springer, Berlin, 2004, and references therein.
[2] S. Moch, P. Uwer, S. Weinzierl, J. Math. Phys. 43 (2002) 3363, hep-ph/0110083.
[3] T. Huber, D. Maitre, Comput. Phys. Commun. 175 (2006) 122–144, hep-ph/0507094.
[4] M.Y. Kalmykov, JHEP 0604 (2006) 056, hep-th/0602028.
[5] I.G. Halliday, R.M. Ricotta, Phys. Lett. B 193 (1987) 241.
[6] C. Anastasiou, E.W.N. Glover, C. Oleari, Nucl. Phys. B 572 (2000) 307, hep-ph/9907494.
[7] A.T. Suzuki, E.S. Santos, A.G.M. Schmidt, Eur. Phys. J. C 26 (2002) 125, hep-th/0205158.
[8] A.T. Suzuki, E.S. Santos, A.G.M. Schmidt, J. Phys. A 36 (2003) 4465, hep-ph/0210148.
[9] A.T. Suzuki, A.G.M. Schmidt, J. Phys. A 31 (1998) 8023.
[10] C. Anastasiou, E.W.N. Glover, C. Oleari, Nucl. Phys. B 565 (2000) 445, hep-ph/9907523.

[11] C. Anastasiou, E.W.N. Glover, C. Oleari, Nucl. Phys. B 575 (2000) 416;
C. Anastasiou, E.W.N. Glover, C. Oleari, Nucl. Phys. B 585 (2000) 763, Erratum.
[12] A.T. Suzuki, A.G.M. Schmidt, Can. J. Phys. 78 (2000) 769, hep-th/9904195.
[13] A.T. Suzuki, A.G.M. Schmidt, JHEP 9709 (1997) 002, hep-th/9709024.
[14] A.T. Suzuki, A.G.M. Schmidt, Eur. Phys. J. C 5 (1998) 175, hep-th/9709144.
[15] A.T. Suzuki, A.G.M. Schmidt, Solutions for a massless off-shell two-loop three-point vertex, hep-th/9712104.
[16] A.T. Suzuki, A.G.M. Schmidt, Phys. Rev. D 58 (1998) 047701, hep-th/9712108.
[17] A.T. Suzuki, A.G.M. Schmidt, J. Phys. A 35 (2002) 151, hep-th/0110047.
[18] I. Gonzalez, I. Schmidt, Phys. Rev. D 72 (2005) 106006, hep-th/0508013.
[19] E.E. Boos, A.I. Davydychev, Theor. Math. Phys. 89 (1991) 1052.
[20] A.I. Davydychev, J. Math. Phys. 32 (1991) 1052.
[21] A.I. Davydychev, J. Math. Phys. 33 (1992) 358.
[22] A.T. Suzuki, A.G.M. Schmidt, J. Comput. Phys. 168 (2001) 207, hep-th/0008143.
[23] R. Hilfer, Applications of Fractional Calculus in Physics, World Scientific, Singapore, 2000.
[24] K.S. Miller, B. Ross, An Introduction to the Fractional Calculus and Fractional Differential Equations, John Wiley & Sons, 1993.
[25] K.B. Oldham, J. Spanier, The Fractional Calculus, Theory and Applications of Differentiation and Integration to Arbitrary Order, Academic Press, 1974.
[26] W.N. Bailey, Generalized Hypergeometric Functions, Cambridge Univ. Press, Cambridge, 1966.
[27] G. Gasper, M. Rahman, Basic Hypergeometric Series, Cambridge Univ. Press, 1990.
[28] L.J. Slater, Generalized Hypergeometric Functions, Cambridge Univ. Press, 1966.
[29] L.S. Gradshteyn, L.M. Ryzhik, Table of Integrals, Series, and Products, sixth ed., Academic Press, 2000.
[30] H. Exton, Multiple Hypergeometric Functions and Applications, Ellis, Harwood, 1976.